การสลายเมทิลีนบลูด้วยตัวเร่งปฏิกิริยาพอลิโดพามีน-Ag/TiO_2 แบบใช้แสง

นางสาวกมลทิพย์ ธรรมารักษ์วัฒนะ

วิทยานิพนธ์นี้เป็นส่วนหนึ่งของการศึกษาตามหลักสูตรปริญญาวิศวกรรมศาสตรมหาบัณฑิต
สาขาวิชาวิศวกรรมเคมี ภาควิชาวิศวกรรมเคมี
คณะวิศวกรรมศาสตร์ จุฬาลงกรณ์มหาวิทยาลัย
ปีการศึกษา 2560

PHOTOCATALYTIC DEGRADATION OF METHYLENE BLUE OVER POLYDOPAMINE-AG/TIO_2

Miss Kamonthip Tammarakwattana

A Thesis Submitted in Partial Fulfillment of the Requirements
for the Degree of Master of Engineering Program in Chemical Engineering
Department of Chemical Engineering
Faculty of Engineering
Chulalongkorn University
Academic Year 2017

Thesis Title	PHOTOCATALYTIC DEGRADATION OF METHYLENE BLUE OVER POLYDOPAMINE-AG/TIO_2
By	Miss Kamonthip Tammarakwattana
Field of Study	Chemical Engineering
Thesis Advisor	Akawat Sirisuk, Ph.D.

Accepted by the Faculty of Engineering, Chulalongkorn University in Partial Fulfillment of the Requirements for the Master's Degree

.....Dean of the Faculty of Engineering

(Associate Professor Supot Teachavorasinskun, D.Eng.)

THESIS COMMITTEE

.....Chairman

(Professor Siriporn Damrongsakkul, Ph.D.)

.....Thesis Advisor

(Akawat Sirisuk, Ph.D.)

.....Examiner

(Chalida Klaysom, Ph.D.)

.....External Examiner

(Assistant Professor Tanawan Pinnarat, Ph.D.)

กมลทิพย์ ธรรมารักษ์วัฒนะ : การสลายเมทิลีนบลูด้วยตัวเร่งปฏิกิริยาพอลิโดพามีน-Ag/TiO_2 แบบใช้แสง (PHOTOCATALYTIC DEGRADATION OF METHYLENE BLUE OVER POLYDOPAMINE-AG/TIO_2) อ.ที่ปรึกษาวิทยานิพนธ์หลัก: ดร.อัครวัต ศิริสุข, 73 หน้า.

งานวิจัยนี้จัดทำขึ้นเพื่อศึกษาผลของการเติมซิลเวอร์ และพอลิโดพามีนบนตัวเร่งปฏิกิริยาไทเทเนียมไดออกไซด์ในการสลายสารละลายเมทิลีนบลูด้วยแสง โดยใช้การเตรียมตัวเร่งปฏิกิริยาไทเทเนียมไดออกไซด์ด้วยวิธีโซลเจล นำไปเผาที่อุณหภูมิ 400 องศาเซลเซียสเป็นเวลา 2 ชั่วโมง แล้วทำการเติมซิลเวอร์ด้วยวิธีการเคลือบฝังแบบแห้งอยู่ในช่วงร้อยละ 0.5 ถึง 3 โดยน้ำหนัก จากนั้นเตรียมพอลิโดพามีนบนตัวเร่งปฏิกิริยาด้วยวิธีการเคลือบฝังแบบเปียก โดยมีโดพามีนเป็นสารตั้งต้นปริมาณพอลิโดพามีนอยู่ในช่วงร้อยละ 5 และ 10 โดยน้ำหนัก ตัวเร่งปฏิกิริยาทั้งหมดในงานวิจัยนี้ถูกนำไปวิเคราะห์เพื่อตรวจสอบคุณสมบัติทางกายภาพและทางเคมีด้วยวิธีการดูดซับด้วยไนโตรเจน ICP-OES XRD FTIR การดูดซับด้วยแก๊สคาร์บอนมอนอกไซด์ Photoluminescence และ UV-Vis spectroscopy ความสามารถของตัวเร่งปฏิกิริยาสำหรับการสลายเมทิลีนบลูถูกทดลองภายใต้แสงยูวีและแสงวิสิเบิล ในแต่ละการทดลองตัวเร่งปฏิกิริยาถูกเติมลงในสารละลายเมทิลีนบลูเข้มข้น 10 ppm ทำการกวนในที่มืดเป็นเวลา 1 ชั่วโมง จากนั้นทดลองภายใต้แสงยูวีและแสงวิสิเบิลเป็นเวลา 2 ชั่วโมง ความเข้มข้นของเมทิลีนบลูถูกวัดด้วยเครื่อง UV-Vis spectroscopy สำหรับประสิทธิภาพของการสลายเมทิลีนบลูของตัวเร่งปฏิกิริยาพบว่า เมื่อมีการเติมซิลเวอร์ และพอลิโดพามีนลงบนตัวเร่งปฏิกิริยาไทเทเนียมไดออกไซด์ ส่งผลให้ประสิทธิภาพของการสลายเมทิลีนบลูของตัวเร่งปฏิกิริยาไทเทเนียมไดออกไซด์มีค่าเพิ่มขึ้นภายใต้แสงยูวี และแสงวิสิเบิล โดยปริมาณซิลเวอร์ร้อยละ 2 โดยน้ำหนัก และพอลิโดพามีนร้อยละ 10 โดยน้ำหนัก ให้ค่าประสิทธิภาพสูงสุดที่ร้อยละ 87.54 ภายใต้แสงยูวี และ 78.98 ภายใต้แสงวิสิเบิล เป็นผลจากบทบาทของซิลเวอร์ในการดักจับอิเล็กตรอน และพอลิโดพามีนในการถ่ายเทอิเล็กตรอน เพื่อช่วยลดการรวมกันของคู่อิเล็กตรอนและโฮล ลดช่องว่างของระดับชั้นพลังงาน และเพิ่มความสามารถในการดูดซับแสงในช่วงวิสิเบิลของตัวเร่งปฏิกิริยา ซึ่งส่งผลให้เกิดการกระตุ้นอิเล็กตรอนจากการดูดซับแสงในช่วงวิสิเบิลเพิ่มมากขึ้น

ภาควิชา วิศวกรรมเคมี ลายมือชื่อนิสิต .....

สาขาวิชา วิศวกรรมเคมี ลายมือชื่อ อ.ที่ปรึกษาหลัก .....

ปีการศึกษา 2560

5970102021 : MAJOR CHEMICAL ENGINEERING
KEYWORDS: : PHOTOCATALYTIC DEGRADATION / POLYDOPAMINE-AG/TIO2 / UV-VISIBLE LIGHT IRRADIATION / METHYLENE BLUE

KAMONTHIP TAMMARAKWATTANA: PHOTOCATALYTIC DEGRADATION OF METHYLENE BLUE OVER POLYDOPAMINE-AG/TIO_2. ADVISOR: AKAWAT SIRISUK, Ph.D., 73 pp.

This research investigated the effect of silver and polydopamine (PDA) doping on TiO_2 catalysts for the photocatalytic degradation of methylene blue in aqueous phase. Titanium dioxide was synthesized via a sol-gel method and was calcined at 400 °C for two hours. Silver was loaded onto TiO_2 by an incipient wetness impregnation method. The amount of Ag was varied from 0.5%wt to 3%wt. Then polydopamine-Ag/TiO_2 catalyst was prepared by an impregnation method, using dopamine as a precursor. The amounts of polydopamine were 5%wt and 10%wt. All catalysts were characterized by N_2 physisorption, ICP-OES, XRD, FTIR, CO chemisorption, Photoluminescence, and UV-Visible spectrophotometry. The photocatalytic degradation of methylene blue in aqueous phase was conducted under either UV or visible light irradiation. In each experiment the catalyst was dispersed in an aqueous solution of 10 ppm methylene blue. The suspension was stirred in the absence of light for one hour and was then irradiated by either one UV or visible light bulb for a period of two hours. The concentration of methylene blue was measured by a UV-Visible spectrophotometer. Addition of both Ag and polydopamine to TiO_2 photocatalyst improved the performance in methylene blue photodegradation under both UV and visible light irradiations. The highest conversion of methylene blue (87.54% under UV irradiation and 78.98% under visible irradiation) was obtained by 10%PDA-2%Ag/TiO_2. Addition of Ag improved trapping of electrons and polydopamine transfered electrons to prevent the recombination of photogenerated charge carriers. Moreover, the band gap was narrower and the light absorption in the visible region was enhanced, leading to more photogeneration of electrons and holes.

Department: Chemical Engineering Student's Signature .....
Field of Study: Chemical Engineering Advisor's Signature .....
Academic Year: 2017

ACKNOWLEDGEMENTS

This thesis would not have been complete without the support of the following individuals. Firstly, I would like to express my profound gratitude to my advisor, Dr. Akawat Sirisuk for his invaluable suggestion, support, and encouragement throughout the entire process of writing this thesis. And I am also very grateful to Professor Siriporn Damrongsakkul, who has been the chairman for her kind supervisor over this thesis, Dr. Chalida Klaysom and Assistant Professor Tanawan Pinnarat, as examiner of the thesis committee for their interest, comments, suggestions and support throughout this thesis.

I would also like to thank several friends at Center of Excellence in Catalysis and Catalytic Reaction Engineering, who always provide the encouragement and assistance along the way.

Finally, I wish to express my profound gratitude to my family for their supports and encouragements throughout.

CONTENTS

Page

Page

Page

LIST OF TABLES

Page

LIST OF FIGURES

Page

CHAPTER I

INTRODUCTION

Over the past few decades, global textile industry including dyeing and printing process has been major sources of residual dye pollutants that are improperly disposed into the environment and are not readily biodegradable. Traditional ways of treatment are classified as biological, physical, or chemical process. Biological treatment, which is beneficial due to its low cost and simplicity, is generally not effective as synthetic dyes are generally resistant to aerobic bio-degradation. Dye removal by physical treatment such as filtration, adsorption or coagulation is usually effective. However, a broad range of wastewater containing dyes cannot be effectively treated by these processes and leads to high operational costs of post treatment of solid and coagulated wastes. Chemical treatment also suffers many drawbacks, such as the production of toxic and carcinogenic by-products, the high dosage of chemicals required, low efficiency, and incomplete mineralization [1, 2]. Since all systems currently need their limitations, development of a significantly improved method of wastewater treatment is of vital for long-term environmental viability of the textile industry. The popular chemical treatment of photocatalytic process using semiconductor has been considered as an eco-friendly and clean technology.

Since the discovery of photocatalytic activity in titanium dioxide (TiO_2) by Fujishima and Honda [3] through their initial work on the photocatalytic splitting of water on TiO_2 electrodes, extensive studies have been done to understand the principles of photocatalysis and to improve the photocatalytic performance of TiO_2 in many applications. In recent years, the widely concerned energy and environment related issues have drawn intense attention onto the application of TiO_2 nanostructures as effective photocatalysts in degrading a wide range of organic pollutants into non-hazardous non-toxic byproducts under UV or visible light irradiation.

Titanium dioxide is one of the most common metal oxides recognized in various industries. Due to its good physical properties, such as catalytic activity, photocatalytic activity, and good stability toward adverse environment. TiO_2 has been used in many fields of application including the use as catalysts, catalyst supports, electronics, cosmetics, pigments and filler coating [4]. Nevertheless, photocatalyst is one of the most important applications of TiO_2. TiO_2 is known to have three natural polymorphus, i.e. rutile, anatase, and brookite, but only anatase is generally accepted to have significant photocatalytic activity.

Several attempts have been made to increase the photocatalytic activity, to extend the light absorption toward the visible light rang, and to prevent the electron recombination of titanium dioxide. Based on the several researches, doping of titanium dioxide with transition metal, loading noble metal, and compounding titanium dioxide with other material have been investigated to raise photocatalytic performance.

Additionally, the presence of noble metals has been reported to enhance the photocatalytic performance of TiO_2. It is believed that photo-generated electrons in the TiO_2 are trapped by the noble metal particles, leading to high efficiency of charge separation [5]. All of the metals, silver is the most attractive dopant in terms of enhancing the photocatalytic activity of TiO_2 and enabling dye degradation because its relatively low price and the ease of the synthesis of Ag/TiO_2. Wodka et al. [6] modified surface properties of the TiO_2 photocatalyst, improves the attraction affinity of cationic dye towards the Ag/TiO_2 surface due to the increased number of electron traps.

More recently, bioinspired polydopamine (PDA) has obtained a wide range of interest due to its unique properties. Polydopamine has revealed remarkable performances in areas such as biosensing, catalysis, and energy storage [7, 8]. Some groups have found out that polydopamine modified titanium dioxide enables the utilization of visible light and can promote the separation of electrons and holes. Furthermore, due to the super-adhesion capabilities of polydopamine, some scientists

have found that it could self-polymerize from dopamine and deposit on the surface of organic and inorganic matter effectively [9].

In previous studies, PDA was coated onto TiO_2 to absorb visible light and applied to dye-sensitized solar cells. Very recently, PDA–TiO_2 core–shell and PDA-nanosphere-modified TiO_2 were introduced into a photocatalytic degradation [10-12]. However, the investigation of TiO_2 catalyst was modified by the optimum amount of metal and polydopamine has not been done before.

In this research, we investigated the photocatalytic degradation of methylene blue in aqueous phase over Ag/TiO_2 catalysts, Titanium dioxide was synthesized via a sol-gel method. The amounts of Ag, varied at 0.5 - 3 %wt, respectively, were loaded on to TiO_2 by an incipient wetness impregnation method. After that, the Ag/TiO_2 catalysts were modified by polydopamine at the amounts of 5 and 10 %wt, respectively. The experiments were conducted under both UV and visible light irradiations.

1.2 Objectives

1. To enhance the efficiency of TiO_2 photocatalytic degradation of methylene blue under UV and visible irradiation using Ag and PDA.

2. To investigate effects of the amount of Ag and PDA addition on properties and photocatalytic activities of PDA-Ag/TiO_2.

1.3 Research scopes

1.3.1 Synthesis of Polydopamine-silver/Titanium dioxide

1. Titanium dioxide (TiO_2) was synthesis by a sol-gel method.

2. Ag/ TiO_2 was prepared by an incipient wetness impregnation method. The amounts of silver was varied from 0.5, 1, 2, and 3 %wt.

3. Polydopamine-Ag/TiO_2 catalyst was prepared by an impregnation method, using dopamine as a precursor. The amounts of dopamine added were 5 and 10 %wt.

1.3.2 The catalyst was characterized by several techniques

1. X-ray diffraction (XRD)

2. Nitrogen physisorption

3. Inductively coupled plasma-optical emission spectroscopy (ICP-OES)

4. CO chemisorption

5. Fourier transform infrared spectroscopy (FTIR)

6. Photoluminescence spectroscopy (PL)

7. UV-visible diffuse reflectance spectroscopy

1.3.3 The photocatalytic activity testing

1. The photocatalytic activity of the catalyst was measured for the photodegradation of methylene blue under either UV or visible light.

2. The concentration of methylene blue from photodegradation was measured by UV-visible spectrophotometer.

Then thesis arranged as follows:

Chapter I presented the introduction an objectives of this study.

Chapter II presented the theory of photocatalytic including basic information about TiO_2 catalyst and principles of photocatalysis.

Chapter III presented the literature review of previous works related to this research.

Chapter IV presented the synthesis of the TiO_2 sol, TiO_2 modified by Ag and PDA, the photocatalytic testing, and characterization techniques in this study.

Chapter V presented the experimental result and discussion.

Chapter VI included the overall conclusion of this research and recommendation for future works.

CHAPTER II

THEORY

The theory relating to overview of titanium dioxide, principle of photocatalytic degradation, and modification of TiO_2 will be explained in this chapter.

2.1 Physical and chemical properties of titanium dioxide

Titanium dioxide (TiO_2), also known as titania, is a widely used multifunctional material because of its physical & chemical properties, its non-toxicity, low cost, relatively high chemical stability and the possibility of using sunlight as a source of irradiation [13]. Therefore it has been used in many fields of application such as catalyst, catalyst support, electronics, cosmetic pigment, and filter coating [14]. Since Fujishima and Honda [3], found the phenomenon of splitting of water on a TiO_2 photocatalyst under UV light. After this, a plenty of efforts have been committed to the study of TiO_2 material, which has developed large number of positive applications in various areas from photovoltaic and photocatalysis to photo-electrochromics and sensors [15]. In recent year, main attention has been devoted to its photocatalytic activity. Titanium dioxide has relatively large band gap of 3.2 eV, charge carriers, i.e. electrons and holes, are produced when titanium dioxide is excited. Consequently, highly active radicals are generated and oxidation-reduction when it was absorbed on surface of titanium dioxide can occur.

Titanium dioxide exhibits three major crystalline phases: rutile, anatase and brookite. Rutile is the most stable phase for small crystals (< 11nm), anatase for large crystals (> 35nm) and brookite in between. Rutile and anatase are the most studied of the phases, particularly in the field of surface science [16-18]. Sclafani et al. [19]

reported that anatase is the most active phase of TiO_2 compared with the amorphous and the rutile phases, whereas brookite is photocatalytically inactive. Rutile is the most thermodynamically stable phase at high temperature. Its structure can be observed at temperature between 673–1073 K [15]. The surface enthalpies of the three crystal structures of TiO_2 are also different. Upon heating, anatase and brookite are observed to form rutile, but also to coarsen, showing the balanced energetics as a function of particle size. The change of thermodynamic stability of the three polymorphous can take place under conditions that prevent coarsening, with anatase and/or brookite being stable at small particle size regimes [20].

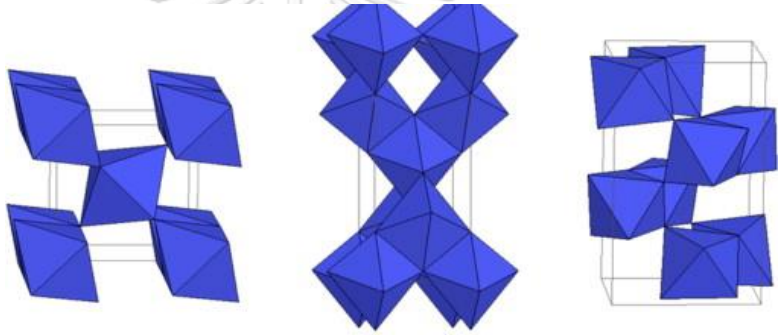

Figure 2.1 Crystal structure of rutile, anatase, and brookite TiO_2 phase [21]

Table 2.1 Properties of Titanium dioxide [22]

Properties of Titanium dioxide (TiO_2)	
Molecular Formula	TiO_2
Molecular Weight	79.866 g/mol
Density	4.24 g/cm^3 (Rutile) 3.77 g/cm^3 (Anatase)
Melting point	1844°C
Boiling point	2973°C
Refractive index(nD)	2.489 (Anatase) 2.584 (Brookite) 2.608 (Rutile)
Appearance	White solid
Solubility	Insoluble in water
Odour	Odourless

2.2 Titanium dioxide synthesis method

There are several methods that can be used to synthesize anatase titanium dioxide. In general, methods which have been reported for anatase synthesis are a sol-gel method. Chemical vapor deposition method, thermal decomposition and precipitation method. The different method can give the different of surface area, phase, pore size and morphologies of the TiO_2. Compare to the other techniques, a sol-gel is mostly used because this method has many advantages such as a possibility of making deposited on complex-shaped substrates, easy control of doping level, simple equipment and inexpensive start-up materials. These include that it can be prepared at room temperature, applied by using ultrasonic spray coater to aid dispersion, obtained high surface area and better thermal stability than stirring method.

2.2.1 Sol-gel method [23]

This method can be performed at relatively low temperature to prepare a solid. Sol is first prepared form suitable reactants in suitable liquid. Sol preparation can be either simply the dispersion of insoluble solids in liquid or addition of precursor which reacts with the solvent to form a colloidal product. A typical example of the former approach is dispersion of oxides or hydroxides in water with the pH adjusted so that the solid particles remain in suspension rather than precipitate out. A typical example of the later approach is the addition of metal alkoxide to water. The alkoxide is hydrolyzed giving the oxide as a colloidal product.

A sol-gel process occurs in liquid solution of organometallic precursor (e.g. titanium isopropoxide), which lead to the formation of sol by means of hydrolysis and condensation reaction.

Scheme 1 The formation of sol-gel process

M-O-R + H_2O	⟶	M-OH + R-OH	Hydrolysis	(2.1)
M-O-H + HO-M	⟶	M-O-M + H_2O	Water condensation	(2.2)
M-O-R + HO-M	⟶	M-O-M + R-OH	Alcohol condensation	(2.3)

A typical example of a sol-gel method is addition of metal alkoxide to water. The alkoxide is hydrolyzed, giving the oxide as colloidal product.

The sol is made of many solid particles suspended in a liquid phase. After that, particles coallesce into gel, in which solid macromolecules are immersed in a liquid phase. Drying the gel at low temperature produces porous solid matrices or xerogels. To obtain a final product, the gel is heated. This treatment serves several proposes, i.e. to remove solvent, to decompose anions such as alkoxides or carbonates to give oxides, it rearrange of the structure of solid, and to allow crystallization to occur.

2.3 Principles of heterogeneous photocatalysis

In chemistry, homogeneous catalysis refers to a series of reactions that are catalyzed by a catalyst in the same phase as the reactants. Usually, homogenous catalysts are dissolved together with the reactants in a solvent, most commonly water. Due to the technically difficult and economically undesirable process of post-reaction separation, heterogeneous reaction is more preferred, where the catalyst is in a different phase with the reactants and is hence more easily to be separated. In general, in order for a heterogeneous reaction to occur.

Five steps are necessary [24]:

(1) Diffusion of reactant molecules from the bulk to the surface

(2) Adsorption onto the surface

(3) Reaction on the surface

(4) Desorption of products from the surface

(5) Diffusion of products to the bulk.

2.3.1 Titanium dioxide photocatalysis

Photocatalysis refers to a reaction when the catalyst is activated by light. During the photocatalytic process, the photocatalytic abilities of TiO_2 are due to the production of excited electron/hole pairs when the material is exposed to UV or visible light. The UV or visible radiation leads to a charge separation due to excitation of an electron (e^-) from the valence band to the conduction band of TiO_2, simultaneously forming a hole (h^+, a region of positive charge density) in the valence band. The mechanism of photocatalysis is illustrated by Figure 2.2 [25].

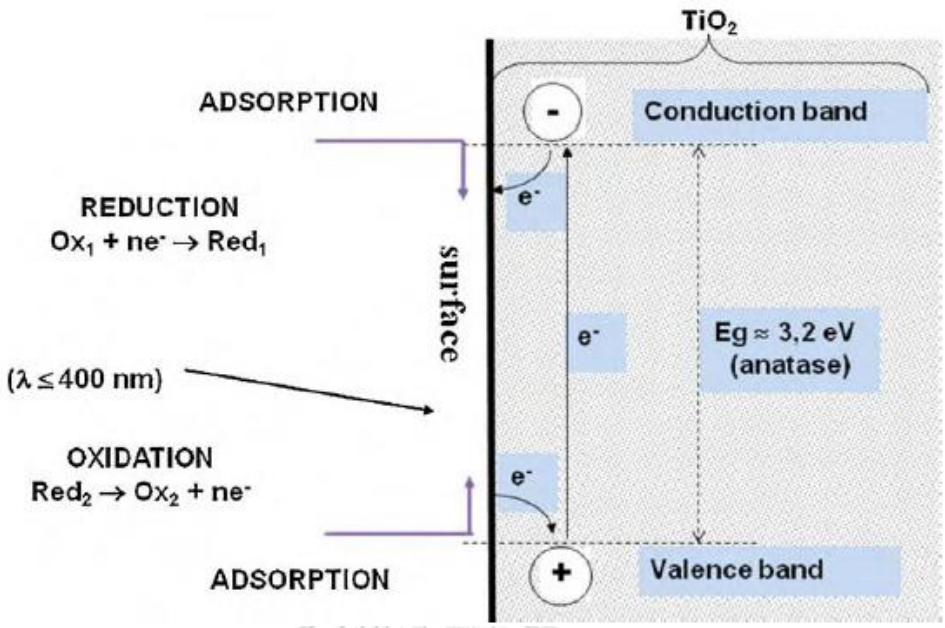

Figure 2.2 Electron energy plotted upwards as a function of the distance from the surface to the bulk of titanium dioxide (E_g is the band gap energy) [22]

As expressed in Scheme 2, this process generates a photoexcited electron and hole (Eq. 2.4). Possible further reactions are represented by Eq. 2.5-2.9, while Eq. 2.10-2.12 represent the possible recombination pathways. Eq. 2.6 and 2.7 illustrate the formation of OH radicals and O vacancies due to competition for holes [26].

Scheme 2 Excitation process of TiO_2 and its further mechanisms [27]

$TiO_2 + h\nu$	⟶	$e^- + h^+$	(2.4)
e^- + Ti(IV)O-H	⟶	$Ti(III)O\text{-}H^-$	(2.5)
h^+ + Ti(IV)O-H	⟶	Ti(IV)O-H	(2.6)
$h^+ + ½\ O^{2-}_{lattice}$	⟶	¼ O_2 (g) + vacancy	(2.7)
e^- + O_2 (surface)	⟷	O_2^- (surface)	(2.8)
$O_2,s^- + H^+$	⟶	HO_2,s	(2.9)
h^+ + $Ti(III)O\text{-}H^-$	⟶	Ti(IV)O-H	(2.10)
e^- + Ti(IV)O-H	⟶	Ti(IV)O-H	(2.11)
O_2^-(surface) + Ti(IV)O-H	⟶	Ti(IV)O-H + O_2 (surface)	(2.12)

Oxidant radical species such as superoxide ($O_2^{\bullet-}$), hydroxyl (OH•), or peroxide (OOH•) may result from redox reactions of the photogenerated electron-hole pairs. These radicals are responsible for the heterogeneous photodegradation of organic substrates such as dyes on the TiO_2 surface. Akpan and Hameed [28] have reported that these radicals will readily oxidize most azo dyes. Reactions relevant to the photodegradation of organic dyes on the surface of TiO_2 are described in Scheme 3.

Scheme 3 Relevant reactions of degradation of dyes at the surface of TiO_2 [29]

$TiO_2(hVB^+) + H_2O$	⟶	$TiO_2 + H^+ + OH^\circ$	(2.13)
$TiO_2(hVB^+) + OH^\circ$	⟶	$TiO_2 + OH^\circ$	(2.14)
$TiO_2(eCB^-) + O_2$ (surface)	⟶	$TiO_2 + O_2^{-\circ}$ (surface)	(2.15)
$O_2^{-\circ}$(surface) + H^+	⟶	HO_2°	(2.16)
Dye + OH°	⟶	degradation products	(2.17)
Dye + hVB^+	⟶	oxidation products	(2.18)
Dye + eCB^-	⟶	reduction products	(2.19)

Most of these degradation reactions occur due to the presence of the hydroxyl radical, which is a very strong oxidizing agent (Eq. 2.17). Dyes that will not

react with the hydroxyl radical can follow either oxidation or reduction pathways as showed by Eq. 2.18-2.19, but these routes are less effective overall.

2.4 Modified titanium dioxide with silver

Silver is of particular interest because of distinctive properties, such as good conductivity, chemical stability, antibacterial and catalytic. The surface modification of TiO_2 photocatalyst by Ag was doping. Doping is a commonly-used method to narrow the band gap and change the electronic properties of TiO_2 [30]. TiO_2 is doped by loading other components, either organic or inorganic, into the bulk material, modifying its optical activity. Doping Ag involves introducing Ag impurity ions on the photocatalytic properties of TiO_2 which has been another interested area of semiconductor modification. The benefit of Ag doping species is the improved trapping of electrons to inhibit electron-hole recombination during illumination [31]. It is believed that these Ag create acceptor and donor centers where direct recombination occurs. Another reason for the improvement of the performance of TiO_2 nanomaterials is to increase their optical activity by shifting the onset of the response from the UV to the visible region. Li et al., (2008) [32] prepared the Ag/TiO_2 by photochemical reduction process under UV irradiation method. The activity of the catalyst was investigated by photodegradation of methyl orange in water. The metallic silver can help the electron-hole separation by attract photoelectron.

2.5 Properties of polydopamine

PDA is a mussel adhesive-inspired biomimetic synthetic polymer with good affinity to almost any solid surface through chemical binding and physical interactions resulting from its diverse functional groups, especially its catechol group [33]. In general, there are three routes to prepare PDA, i.e., enzymatic catalytic oxidation, electrochemical polymerization (on an electrically conductive electrode), and oxidation polymerization in solutions [34]. Solution oxidation is the most popular method because the oxidation polymerization of dopamine (DA) can be conveniently conducted at room temperature in basic aqueous solutions, forming a PDA coating on

various substrates. In the presence of laccase and at a pH of about 8.5, DA can be oxidized and then polymerizes into PDA.

PDA has gained a wide range of interest in functionalizing the surface of biomaterials as well as in different fields such as in lithium ion batteries, supercapacitors, transparent conductive electrodes and photoelectrochemical electrodes, and catalysis of the oxygen reduction reaction [35, 36]. PDA possesses a good UV and visible-light-absorption ability and good photoconductivity under visible-light irradiation, leading to an increase of photogenerated charge carriers due to its polymeric **π**-conjugated structure leading to electrical conduction capability [37]. In addition, PDA, contains an amount of catechol groups, and under neutral and basic conditions, it has semiquinone or quinone groups; thus, it can accept electrons and protons from an electron donor. Therefore, PDA can effectively transfer and separate photoinduced electrons and protons as an electron gate for artificial photocatalysis systems, which will effectively avoid the electron–hole recombination of semiconductor photocatalysts and improve photocatalytic activity.

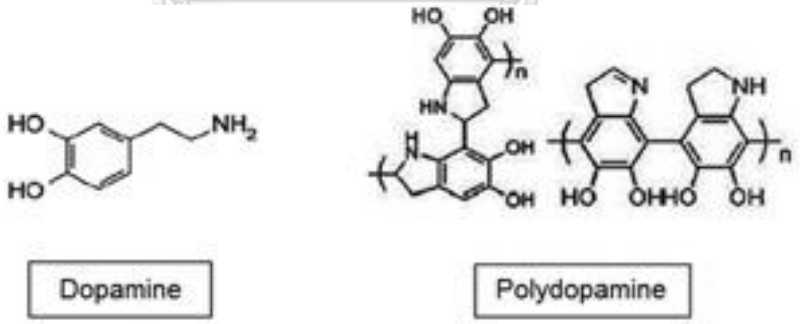

Figure 2.3 Structures of dopamine and polydopamine [38]

2.6 Methylene blue [39]

Methylene blue is cationic dye used in industries such as the textile industry for a variety of purposes. It is a heterocyclic aromatic chemical compound with a molecular formula $C_{16}H_{18}N_3SCl$.

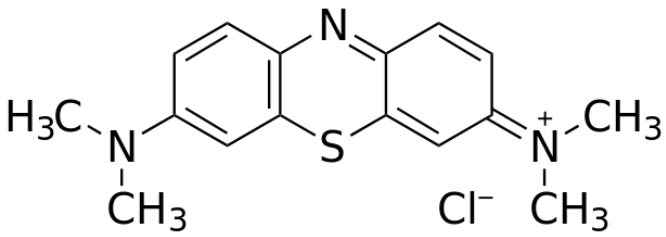

Figure 2.4 Structure of methylene blue [39]

This dye gives a blue solution when mixed with water, and has been reported to be toxic or induce endocrine disruption in aquatic organisms when persistent in water. Throughout a chemical or biological reaction pathway, these dye compounds not only deplete the dissolved oxygen in water bodies, they also release toxic compounds that threaten aquatic life. It can also cause eye burns which may be responsible for permanent injury to the eyes of both human and animals. Upon inhalation, it can give rise to short periods of rapid or difficult breathing whereas ingestion through the mouth causes gastrointestinal tract irritation, producing a burning sensation and may cause nausea, vomiting, profuse sweating, and mental confusion.

CHAPTER III

LITERATURE REVIEWS

This chapter contains a survey of several studies involving modified titanium dioxide and other catalysts with Ag and polydopamine. This section discusses the effects of Ag and polydopamine addition to titanium dioxide photocatalyst. Including photocatalytic activity on photocatalytic degradation for water purification.

3.1 Effects of silver added to titanium dioxide on properties and photocatalytic activities

Jiang et al. [40] studied the visible-light-driven one-dimensional (1D) anataseTiO_2/Ag plasmonic photocatalyst. One-dimensional (1D) anataseTiO_2/Ag was successfully prepared through a facile wet impregnation method. Experimental results indicate that Ag nanoparticles cover on the surface of TiO_2 uniformly and the heterogeneous structure is formed efficiently. The obtained 1D anatase TiO_2/Ag heterogeneous composites exhibit excellent photocatalytic activity (nearly 100% within two hours) for degradation of 2,4-dichlorophenol in wastewaters under visible-light irradiation, which is ascribed to the suitable particle size of Ag nanoparticles in favor of enhancing the surface plasmon resonance and the heterogeneous structure advantageous of the separation of photogenerated electron–hole pairs. After reusage for ten times, the composites still present high photocatalytic activity, indicating the excellent stability.

Lee et al. [41] studied the nano Ag/TiO_2 catalyst prepared by chemical deposition and its photocatalytic activity. Silver nanoparticles were synthesized and cetyltri- methyl ammonium bromide was used as the surfactant to disperse Ag particles in water, Ag particles were then deposited on TiO_2. The photocatalytic reaction of these catalysts for methylene blue destruction was carried out in a batch reactor under UV light irradiation. The results showed that Ag particles were finely dispersed and

homogeneously distributed on TiO_2 support and had strong metal support interaction with TiO_2 by using chemical deposition method. Large amount of hydroxyl groups were on the surface of the catalysts. The photocatalytic activity increased after loading with Ag. Ag particles offered electron traps to decrease the recombination of electrons and holes, but too many Ag nanoparticles block the TiO_2 surface from light scattering. The optimum Ag loading was 2 wt%.

Kong et al. [42] studied enhanced visible-light-active photocatalytic performances on Ag nanoparticles sensitized TiO_2 nanotube arrays. TiO_2 nanotube arrays (TNAs) synthesized using anodic oxidation method perform an excellent photocatalytic activity due to their unique tubular structure and large specific surface areas. Ag nanoparticles sensitized TiO_2 nanotube arrays (Ag/TNAs) were synthesized using classical anodic oxidation methods and special hydrothermal methods. The result showed that Ag nanoparticles were well-dispersed and anchored to the top surface of TNAs. UV–vis absorption spectra performed an enhanced absorbance to visible light and photoluminescence performed a better optical property than pure TNAs. The photocatalytic performances of the as-synthesized Ag/TNAs were evaluated in terms of their photodegradation rate of methylene blue in an aqueous solution under light. The Ag/TNAs showed an enhanced photocatalytic activity compared with pure TNAs, and a probable photocatalytic mechanism was proposed.

3.2 Effects of polydopamine added to titanium dioxide on properties and photocatalytic activities

Gaham et al. [43] studied dopamine self-assembled functionalization bestows trititanate nanotubes with stable, recyclable photocatalytic activity under UV and visible light illumination. The result showed that this activity owed to electron transfer between the nanotubes and dopamine, as exhibited in the photoluminescence quenching of the modified tubes, which resulted in longer charge-separation and allowed the adsorbed dye to be degraded. The controlled surface modification enabled the harvesting of visible light. The recyclable photocatalytic degradation of

adsorbed dye showed the dopamine-modified trititanate nanotubes absorbed and degraded all of the dye in each cycle, thereby showing the stability of the composite.

Huaiyuan et al. [44] studied polydopamine-modified Ag/TiO_2 porous nanofibers (PDA-Ag/TiO_2 porous NFs). The PDA-Ag/TiO_2 porous NFs were successfully prepared as a composite catalyst via a simple electrospinning process combined with an impregnation method. It was found that the PDA-Ag/TiO_2 porous NFs present a corn-like, coarse, porous structure where the TiO_2 NFs look like corn cobs and the Ag nanoparticles (NPs) act as corn kernels. The results of the photodegradation of methyl orange using ultraviolet light showed that the corn-like PDA-Ag/TiO_2 NF composite catalyst exhibits high-efficiency photocatalytic activity. They could detect that the porous TiO_2 nanofibers fabricated using the pore-forming of carbon nanotubes have a higher specific surface area than pure TiO_2. This property gives the TiO_2 NFs a better adsorption performance which is beneficial for photodegradation. In addition, Ag and PDA can greatly improve the photocatalytic performance cooperatively.

Xiaosong et al. [11] studied the dramatic visible light photocatalytic activity was obtained for the degradation of methyl orange (MO) using TiO_2 photocatalysts modified with polydopamine (PDA) nanospheres. TiO_2/PDA nanocomposites showed absorption in the visible light region, which favors the photocatalytic activity of TiO_2 under visible light. As expected, the TiO_2/PDA nanocomposites exhibit better photocatalytic activity in the photocatalytic degradation of MO under sunlight compared with PDA and TiO_2; this is due to the synergetic effect between TiO_2 and PDA.

Wen-Xin et al. [10] studied the core–shell structured TiO_2/ PDA has been developed to facilitate its application as a photocatalyst. By means of a facile solution based synthesis route, a uniform and conformal PDA nanoshell, which is formed by the in situ polymerization of dopamine (DA), (vary amounts of DA at 0.05, 0.1, 0.2 mmol), is deposited onto the TiO_2 substrate with the coating thickness being readily tuned. Detailed investigation identified that a 1 nm PDA surface coating exhibits relatively high conversion efficiency of solar energy for the photodegradation of organic dyes compared with conventional photocatalysts under visible light irradiation.

Furthermore, the novel core–shell structure can be synthesized easily and on a large scale.

Sujeong et al. [45] TiO_2 complexed with dopamine-derived polymers and the visible light photocatalytic activities for water pollutants. Dopamine (DA) and its derivatives (norepinephrine (NE) and nitrodopamine (NDA) were chosen as monomers, and their polymers (PDA, PNE, and PNDA) were synthesized and subsequently complexed with TiO_2. Visible light-induced catalytic transformations were successfully demonstrated for the reduction of Cr (VI) to Cr (III), dechlorination of CCl_4, oxidation of As (III) to As (V), and H_2O_2 production via dioxygen reduction using polymer-complexed TiO_2. PDA–TiO_2 exhibited the highest activities, which indicates that the polymerized form of DA forms a stronger and more efficient surface complex on the TiO_2 surface for visible light sensitization. DA-derived polymers could efficiently transfer electrons to the TiO_2 conduction band under visible light to initiate reductive transformations, whereas the oxidative transformation of organic substrates was largely inhibited because the organic polymer layer on TiO_2 should scavenge any oxidizing radical species. PDA and PNE exhibited far higher activity than PNDA due to the extensive **π**-electron delocalization induced by the 5, 6-dihydroxyindole structure. This was also supported by the higher photon-to-current conversion and lower charge transfer resistance obtained with PDA–TiO_2 and PNE–TiO_2 (compared with PNDA–TiO_2), which was observed with photoelectrochemical measurements. PDA should be an attractive visible light sensitizer for aquatic transformations.

Zongxue et al. [46] studied the polydopamine/ graphitic carbon nitride (PDA/g-C_3N_4) has been synthesized by the dopamine (DA) polymerization modification of the surface of g-C_3N_4. PDA plays multiple roles as a light absorption substance, an electron transfer acceptor, and an adhesive interface in the design of PDA/g-C_3N_4 photosynthetic systems. The PDA has an effect on the PDA/g-C_3N_4 composite light-harvesting capacity. With an increasing PDA ratio, the photocatalyst's light-harvesting ability was gradually improved. In addition, the 10%PDA/g-C_3N_4 composite has been showed to be highly efficient for the degradation of the organic dyes methylene blue (MB), Rhodamine B

(RhB), and phenol under visible-light irradiation. The degradation efficiency of MB is about 98% in 3 hours, and the catalysts can have a degradation efficiency higher than 90% after four cycles (figure 3.1). The degradation efficiency after four cycles of catalyst showed the PDA wasn't degraded by g-C_3N_4 catalysts in photocatalytic degradation process. PDA, as a surface-modified additive with abundant semiquinone and quinone functional ligands, was introduced for an improvement of the transfer ability of photoinduced electrons and accepts them from a semiconductor-based photocatalysis material (g-C_3N_4), which can reduce electron–hole recombination of g-C_3N_4 and enhance the photocatalytic activity.

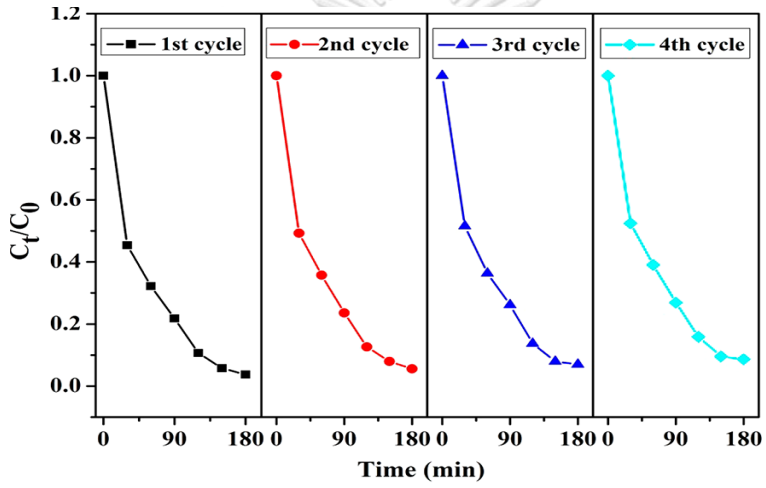

Figure 3.1 Recycling photocatalytic tests of 10%PDA/g-C_3N_4 for the degradation of MB under visible-light irradiation (2 mL, 30 wt% H_2O_2).

Loget et al. [47] studied the highly controlled coating of biomimetic polydopamine (PDA) in TiO_2 nanotubes (TiO_2 NTs). Highly controlled coating of PDA was achieved on TiO_2 NTs by exposing TiO_2 NT arrays to a slightly alkaline dopamine solution. The PDA thin films sensitized the TiO_2 NT arrays and were used for absorption in visible light for enhancing photocurrents and photodegradation. PDA could enhance the photodegradation rates and photocurrents in the visible solar spectrum due to its **π**-conjugated structure (alternate single and double bonds) lead to electrical conduction capability. PDA was furthermore used as a platform for decorating the TiO_2 NTs with different materials such as Ag NPs and Pt NPs. These decorations improved the photoelectrochemical performances of the arrays at a low over potential.

CHAPTER IV

EXPERIMENTAL

This chapter referred to all methods in this research. The experiments involved in 3 sections: (i) preparation of Ag/TiO_2 catalyst that was modified by polydopamine (ii) photocatalytic Experiments, and (iii) physical and electrochemical characterization.

4.1 Preparation of Ag/TiO_2 catalyst that was modified by polydopamine

The preparation of Ag/TiO_2 catalyst that was modified by polydopamine (PDA) can be operated by following these 3 steps. The first step was the preparation of TiO_2 sol via sol-gel method, the second step, Ag was loaded onto TiO_2 by an incipient wetness impregnation method, and the third step, polydopamine-Ag/TiO_2 catalyst was prepared by an impregnation method, using dopamine as a precursor.

4.1.1 Preparation of TiO_2 sol

Titanium dioxide was synthesized via a sol-gel method. Titanium isopropoxide (TTIP) was poured into deionized water (DI) containing a measure amount of 65% nitric acid. The volume ratio of DI: HNO_3: TTIP is 12: 0.088: 1. After the addition of TTIP, white precipitate was formed instantaneously. The mixture was stirred for 3 days until clear sol was obtained and then clear sol was dialyzed in cellulose membrane with MW cutoff of 3500. The distilled water used in dialysis was changed daily until a pH of sol reached 3.5. Finally, the sol was dried and calcined at 400 ℃ for two hours.

4.1.2 Preparation of Ag/TiO_2

The Ag/TiO_2 catalyst was prepared by an incipient wetness impregnation method. A desired amount of $AgNO_3$ was dissolved in DI water and was loaded onto TiO_2 in order to obtain silver at 0.5 to 3 %wt, respectively. The catalyst was dried and then was calcined at 400 °C for two hours.

4.1.3 Synthesis of PDA-Ag/TiO_2 catalyst

First, desired amounts of Ag/TiO_2 and dopamine hydrochloride (i.e., to obtain 5 and 10 %wt of PDA) were added to 100 mL of DI water. The mixture was stirred at a room temperature for 30 minutes. After that, 100 mL of tris-buffer solution (10 mM) was added and the pH of the mixture solution was adjusted to 8.5 using NaOH solution. The mixture was stirred at 60 °C for 12 hours. Then the mixture was cooled down to a room temperature and was centrifuged under 2000 rpm for 20 minutes. The solid was rinsed with DI water three times and the collected solid was dried at 110 °C.

4.2 Photocatalytic experiments

The photocatalytic activity of the catalyst was measured for the photodegradation of methylene blue under UV and visible light irradiations at an ambient temperature. Initially, 0.4 g of catalyst was added to 400 mL of an aqueous solution of 10 ppm methylene blue. The mixture was stirred in the absence of light for one hour to obtain adsorption equilibrium. After that the mixture was exposed to either UV irradiation using 75W UV-C lamp (Philips) or visible light irradiation using 18W TL-D Standard Colors lamp (Philips). During 120 minutes of irradiation, 4 mL of the solution was extracted every 15 minutes to measure the concentration of methylene blue using UV-visible spectrophotometer. The percentage of degradation was calculated by using the equation given below:

$$\%\text{degradation} = \frac{[\text{dye}]_0 - [\text{dye}]_t}{[\text{dye}]_0} \times 100\% \qquad (4.1)$$

In which $[dye]_0$ is the initial dye concentration and $[dye]_t$ is the concentration after the treatments.

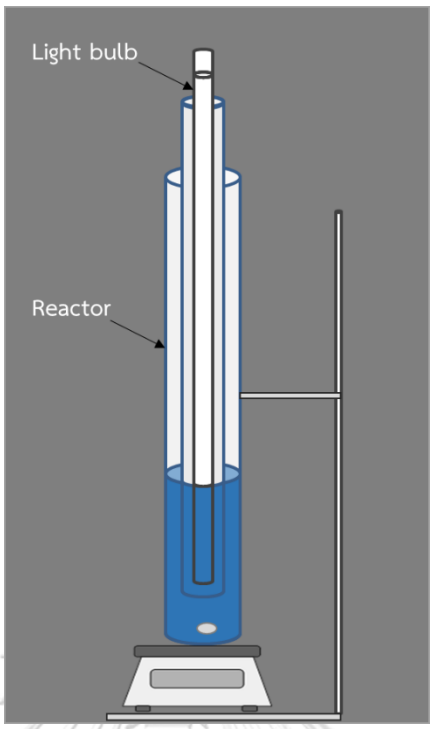

Figure 4.1 Photoreactor set for experiments

4.3 Physical and electrochemical characterization

Several techniques of characterization have been used in this work including physical and electrochemical properties of catalysts.

4.3.1 X-ray diffractometry (XRD)

XRD was performed to determine crystalline phase and crystallite size of TiO_2, Ag/TiO_2 and $PDA\text{-}Ag/TiO_2$. It was conducted using a SIEMENS D5000 X-ray diffractometer with Cu Kα radiation (λ=1.54439 Å) with Ni filter. The spectra were scanned at a rate of 0.04 min^{-1} in the 2θ range of 20-80°.

4.3.2 Nitrogen physisorption

The BET surface area of the catalysts was measured, using Micromeritics ASAP 2020 surface area analyzer. Approximately 0.05 g of the catalysts was placed inside the tube. The sample of catalyst was degassed at 200 °C for one hour.

4.3.3 Fourier trasform infrared (FTIR) spectra

Fourier transform infrared (FTIR) spectra was performed to determine function groups of the catalysts were obtained from an ATR-FTIR spectrometer at number of scan was 300 in wavelength 400-4000 nm, using Thermo Scientific Nicolet 6700 FT-IR spectrometer. The absorbance spectrum shows the various absorbance peaks and these peaks on the spectrum represent functional groups.

4.3.4 UV-Visible spectroscopy (UV-Vis)

The concentration of methylene blue was measured by Perkin Elmer Lambda 650 spectrophotometer at the wavelength of 664 nm and the concentration of polydopamine was measured at the wavelength of 280 nm. To study the light adsorption behavior of the catalysts, the absorbance spectra of the catalyst in wavelength range of 200-800 nm were obtained using by Perkin Elmer Lambda 650 spectrophotometer. The step size for the scan was 1 nm and the band gap of sample was determined by following equation:

$$E_g = \frac{1240}{\lambda} \qquad (4.2)$$

Where E_g is band gap (eV) of the sample, λ (nm) is the wavelength of the onset of spectrum. (The calculation showed in appendix H)

4.3.5 Inductively couple plasma-optical emission spectroscopy (ICP-OES)

The amount of Ag deposited on the surface of titanium dioxide (TiO_2) was measured by inductively-coupled plasma optical emission spectroscopy using the Optima 2100 DV spectrometer. A powder of catalyst was digested into solution phase. Firstly, we dissolved approximately 0.05 g of catalyst into 7 ml of 97% H_2SO_4 acid. Next, 2.7 g of $(NH_4)2SO_4$ was added into solution while being stirred until homogeneous solution was obtained. Then the homogeneous solution was made up to 100 ml with DI water. The diluted solution was measured and compared with a calibration curve of standard solution to obtain an amount of silver loading.

4.3.6 CO-pulse chemisorption

The relative percentages dispersion of Ag supported catalysts were determined by CO-pulse chemisorption technique using Micromeritics ChemiSorb 2750 (pulse chemisorption system). Approximately 0.05 g of catalyst was filled in u-tube, incorporated in a temperature-controlled oven and connects to a thermal conductivity detector (TCD). Then helium (He) was pursed into the reactor with a flow rate 25 ml/min in order to remove remaining air. Prior to chemisorption, the catalyst was reduced in H_2 flow rate 25 ml/min at 550 °C for 1 hours. After being cooled down to room temperature under Helium flow, CO is pulsed into the catalyst bed at 30 °C 20 µl. The non-adsorbed CO was measured using thermal conductivity detector. Pulsing was continued until no further CO adsorption is observed. The relative percentage dispersions of Ag were calculated from CO adsorbed based on CO: Ag ratio of 1:1.

4.3.7 Photoluminescence (PL)

To study the recombination of electrons-holes, photoluminescence measurement was carried out on Fluorescence spectrophotometer (Horiba Fluoromax Spectrofluorometer) at Center of Nanoscience and Nanotechnology, Faculty of Science, Mahidol University by using a Xenon lamp as the excitation source at room temperature. The excitation wavelength used in photoluminescence (PL) measurement was 325 nm.

CHAPTER V

RESULTS AND DISCUSSION

The results and discussion in this chapter are classified into two major parts. In the first part, several characterization techniques for the catalysts including XRD, BET, ICP-OES, FT-IR, CO-chemisorption, PL, and UV-vis are described. And the photocatalytic activity measurements for photocatalysts in the photocatalytic degradation of methylene blue will be discussed in the last section.

5.1 Characterization of the catalysts

5.1.1 The phase structure

The phase structure of catalysts was determined using XRD technique. Figure 5.1 displayed XRD patterns of catalysts with different amount of silver and Figure 5.2 showed XRD patterns of 0.5-3 %wt Ag/TiO_2 with different amount of polydopamine. For all of catalysts, the diffraction peak was be observed at 2θ of 25.37°, 37.86°, 38.61°, 48.12°, and 75.0° corresponding to titanium dioxide anatase phase, diffraction peak at 2θ of 27.48°, 56.65°, 64.2°, and 68.79°, corresponding to titanium dioxide rutile phase and brookite phase shows at 2θ of 30.63° [48, 49]. However the diffraction peak of silver was not observed probably because the low amount of silver [50]**.** The crystallite sizes of the catalyst were calculated using Debye-Scherer equation (in appendix C) and listed in Table 5.1. The crystallite size of pure TiO_2 was 8.9 nm and modification of the catalyst with Ag and PDA showed the crystallite size hardly changed from pure TiO_2**.**

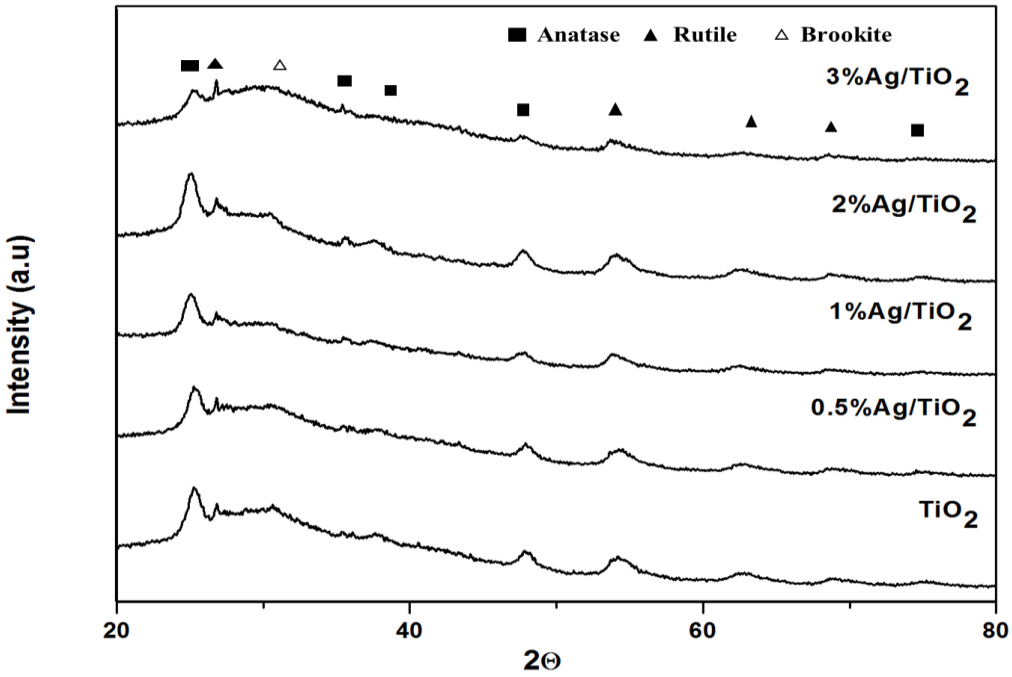

Figure 5.1 XRD patterns of TiO_2 and Ag/TiO_2 catalysts

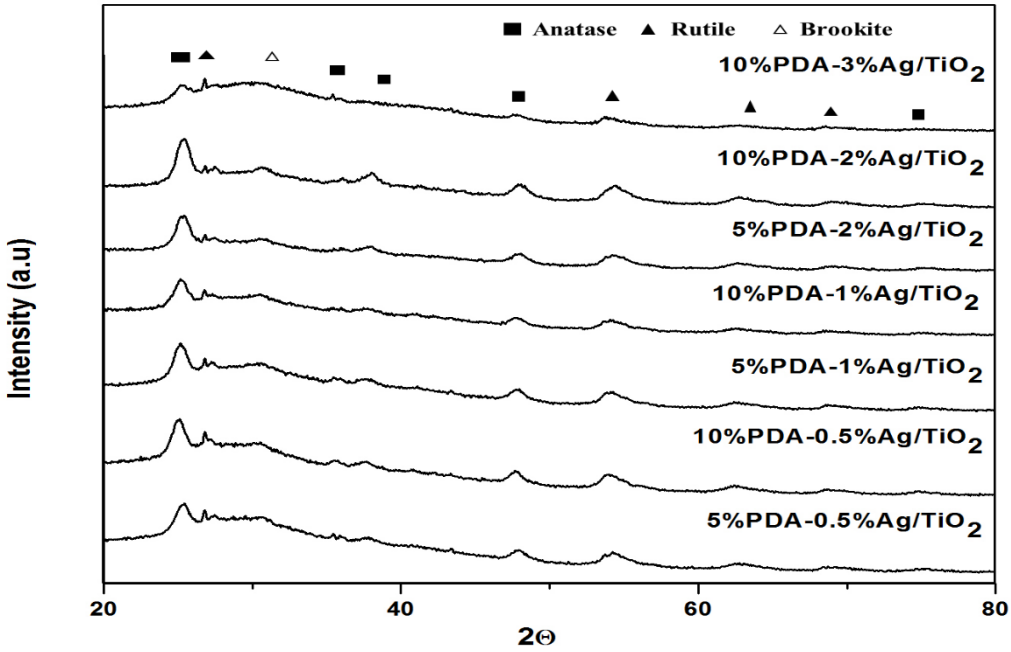

Figure 5.2 XRD patterns of Ag/TiO_2 catalysts that were modified by 5 or 10 %wt PDA

5.1.2 Measurement of specific surface area

The specific surface areas of all TiO_2 and modified TiO_2 were determined from BET adsorption isotherms and are listed in Table 5.1.

Table 5.1 BET surface area, crystallite size, and amount of Ag from ICP of the catalysts calcined at 400°C for 2 hours

Sample	Surface Area (m^2/g)	Crystallite size (nm)	Amount of Ag from ICP (%wt.)
TiO_2	131.47	8.9	-
0.5%Ag/TiO_2	78.04	8.5	0.37
1%Ag/TiO_2	94.81	8.7	0.63
2%Ag/TiO_2	107.75	9.1	1.41
3%Ag/TiO_2	97.27	10.0	2.28
5%PDA-0.5%Ag/TiO_2	87.59	8.4	0.31
10%PDA-0.5%Ag/TiO_2	80.62	9.1	0.32
5%PDA-1%Ag/TiO_2	81.85	8.6	0.62
10%PDA-1%Ag/TiO_2	71.91	9.3	0.67
5%PDA-2%Ag/TiO_2	103.22	7.8	1.47
10%PDA-2%Ag/TiO_2	87.89	8.2	1.31
10%PDA-3%Ag/TiO_2	90.47	8.3	2.38

The results showed that pure TiO_2 possessed the largest specific surface area. Upon addition of Ag, the specific surface area of the catalyst was decreased, because of the second calcination cause the further sintering of pore [51]. Specific surface area of different Ag loading showed around 71-108 m^2/g. The 2%Ag/TiO_2 catalyst showed the largest specific surface area among the four samples of Ag loading. This phenomenon can be explained that Ag are smaller than TiO_2 when content of Ag is small and these Ag load on the surface of TiO_2 resulting in surface area increase. As content of Ag increases gradually, Ag could aggregate into bigger particles which have opposite effect [52]. Furthermore, Addition of PDA loading tended to decrease the

specific surface area of the Ag/TiO_2, suggesting that the coverage of PDA prevented N_2 probe molecule from entering the pores.

5.1.3 Determine of silver content

The amount of silver deposited on titanium dioxide catalysts was measure by inductively-coupled plasma optical emission spectroscopy (ICP-OES). The results are listed in Table 5.1. As see in the results, the actual silver contents determined that was ICP-OES was lower than the expected silver content that was possibly due to incomplete digestion of solid sample with sulfuric acid solution.

5.1.4 CO chemisorption

The amounts of active Ag particles in the present of Ag/TiO_2 and PDA-Ag/TiO_2 catalysts surface with various amount of Ag and PDA were based on the assumption that one carbon monoxide molecule adsorbs on one Ag site (The calculation see in appendix F). The results were showed in Table 5.2. The results showed the low dispersion because CO adsorbs weakly and endothermically on Ag [53]. From the results, the number of Ag active sites and %Ag dispersion tended to decrease when increase amount of silver loading due to more content of silver loading could aggregate to bigger particle so the Ag surface for adsorption decreased. At 2%wt Ag loading showed the lowest Ag dispersion and Ag active site among of four silver loading and when PDA was added, the Ag dispersion hardly decrease.

Table 5.2 Ag Dispersion (%) of Ag/TiO_2 catalysts at various percentages

Sample	Ag active sites (Molecule of CO x $10^{17}/g_{catalyst}$)	Ag Dispersion (%)
0.5%Ag/TiO_2	9.40	4.55
1%Ag/TiO_2	6.75	1.92
2%Ag/TiO_2	5.74	0.73
3%Ag/TiO_2	13.49	1.06
5%PDA-2%Ag/TiO_2	5.99	0.73
10%PDA-2%Ag/TiO_2	5.19	0.71

5.1.5 FTIR analysis

The FT-IR spectra of TiO_2 and various amounts of silver and polydopamine loading on TiO_2 were investigated by Fourier transform infrared spectroscopy with an absorbance mode. The results are showed in Figure. 5.3–5.5. The band at wavenumbers of 600-710 cm^{-1} was attributed to Ti-O-Ti stretching vibration in the TiO_2 lattice, which was observed in every sample. The bands observed at 2000 cm^{-1} and around 2200-2400 cm^{-1} were characteristic of C-H stretching vibrations of molecules with long alkyl chains and C=O bonds showed that the remaining of isopropyl alcohol [54, 55]. When Ag/TiO_2 was modified with PDA (figure. 5.4-5.5), the peaks at 1150, 1200, 1350, and 1750 cm^{-1}, corresponding to C-O, C-NH_2, C-O-H, and aromatic C-C bonds, respectively, were more pronounced due to the presence of PDA [56, 57]. Figure 5.6 showed the higher PDA peak when increased the PDA loading.

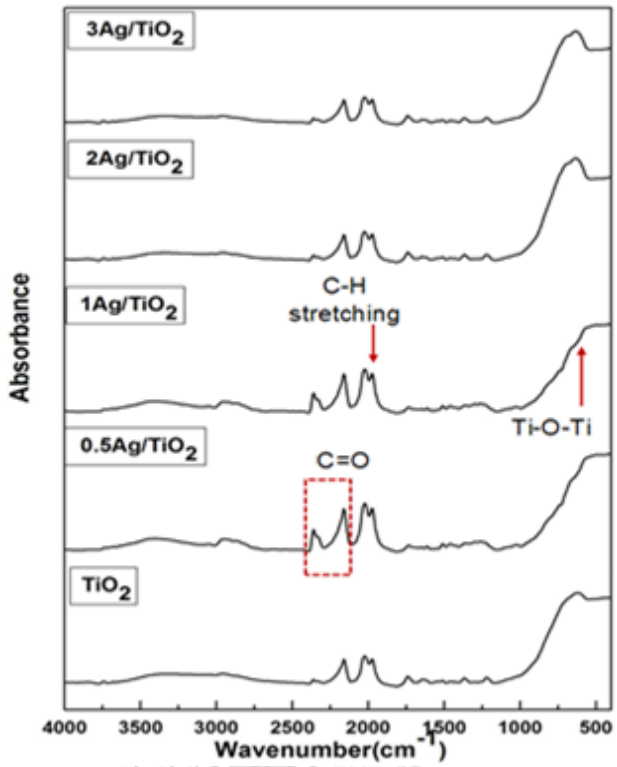

Figure 5.3 FT-IR spectra of TiO_2 and Ag/TiO_2 catalysts at various percentages

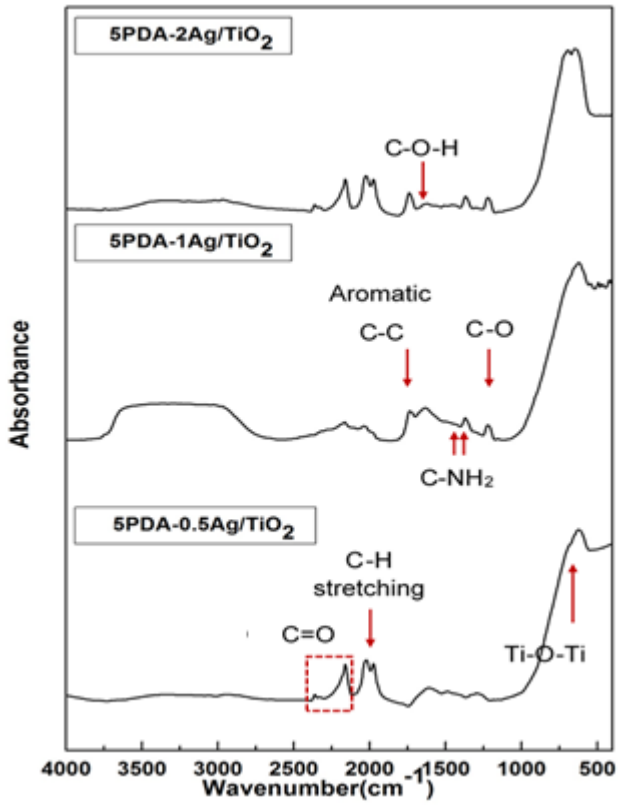

Figure 5.4 FT-IR spectra of 5% PDA-Ag/TiO_2 at various Ag percentages

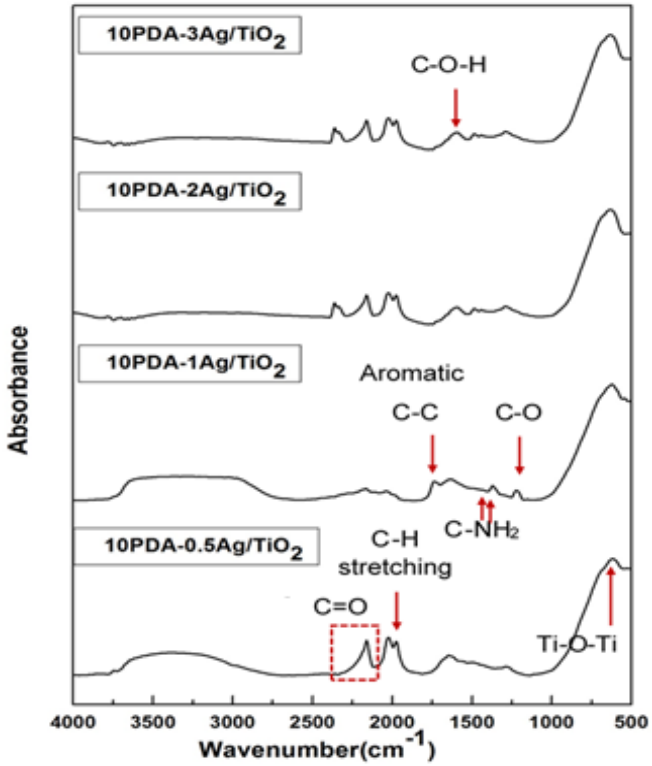

Figure 5.5 FT-IR spectra of 10% PDA-Ag/TiO_2 at various Ag percentages

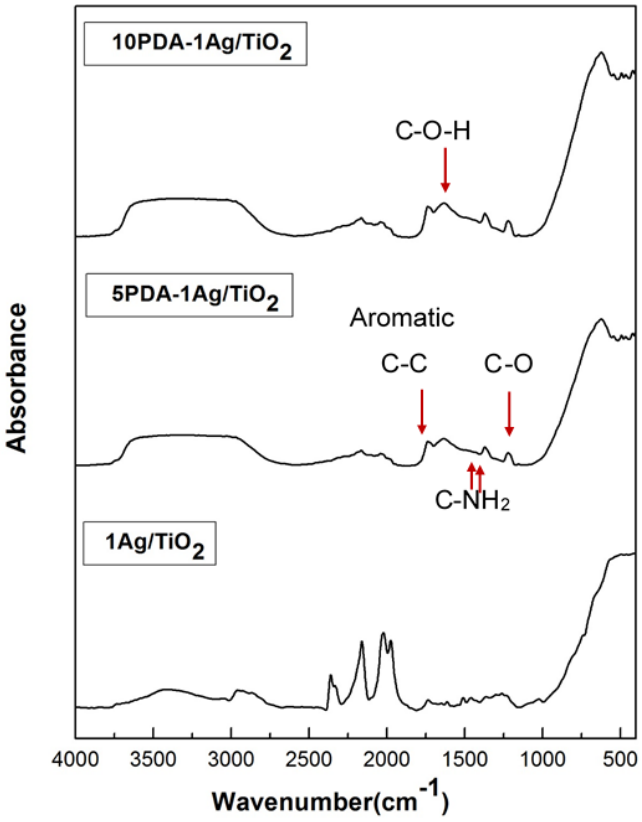

Figure 5.6 FT-IR spectra of 2% Ag/TiO_2 that was modified by 5 or 10 %wt PDA

5.1.6 Determine of polydopamine content

The amount of polydopamine deposited on various silver/titanium dioxide catalysts was measured by UV-visible spectroscopy using wavelength 280 nm. A powder of catalyst was digested into solution phase. Firstly, we dissolved approximately 0.05 g of catalyst into 10 ml of 97% H_2SO_4 acid. While being stirred until the color of solution was changed. Then the resulting solution was made up to 100 ml with deionized water. The solution is ready to measure and compare with a calibration curve to obtain an amount of polydopamine loading. The standard preparation and calibration curve of PDA were showed in appendix G. The amount of polydopamine deposited on various silver/titanium dioxide was showed in Table 5.3. The result showed that the real content of PDA was lower than the expected PDA content that was due to incomplete dissolution of polydopamine from catalysts.

Table 5.3 The amount of polydopamine deposited on various silver/titanium dioxide catalysts

Sample	Amount of PDA (%wt)
5%PDA-0.5%Ag/TiO_2	3.95
10%PDA-0.5%Ag/TiO_2	7.90
5%PDA-1%Ag/TiO_2	4.54
10%PDA-1%Ag/TiO_2	8.39
5%PDA-2%Ag/TiO_2	4.22
10%PDA-2%Ag/TiO_2	7.96
10%PDA-3%Ag/TiO_2	8.09

5.1.7 UV-visible absorption spectra

To assess the optical absorption properties of the catalyst, UV visible spectroscopy was conducted in the range of 200 to 800 nm. As showed in Fig. 5.7 (a), TiO_2 does not absorb any light in the visible region (greater than 400 nm). When Ag was doped into the TiO_2, the visible light response was improved and increasing Ag content, the catalysts had gradually higher absorption in the visible light (see Fig.5.7

(b-e)). Moreover, PDA modification has a considerable influence on the optical property of PDA-Ag/TiO_2. An increase in PDA in the catalyst gave rise to a drastic increase in the absorption of light in the visible-light region, suggesting that the PDA-Ag/TiO_2 possesses a potential to harvest more visible light than pure TiO_2 and Ag/TiO_2.

The band-gap energy of the catalyst was estimated from Figure 5.8-5.10 and was displayed in Table 5.4. The band-gap energies of TiO_2, were 3.2 eV. When various Ag was dope the band gap slightly narrowed. When adding PDA on various Ag/TiO_2 showed the significantly decreased band gap because PDA has **π**-conjugated structure lead to PDA was able to absorb light in the visible-light region. As the amount of PDA increased, the band gap of the catalyst became narrower. The narrowing of the band gap suggested that PDA-Ag/TiO_2 composite was able to absorb light with longer wavelength, compared to TiO_2. Consequently, the composite would exhibit a better performance in photocatalytic degradation of dye. For the comparison band gap as showed in Table 5.4, which the Ag and PDA doping has the reduced band gap energy. Thus, the Ag and PDA doping effect to the activated visible region.

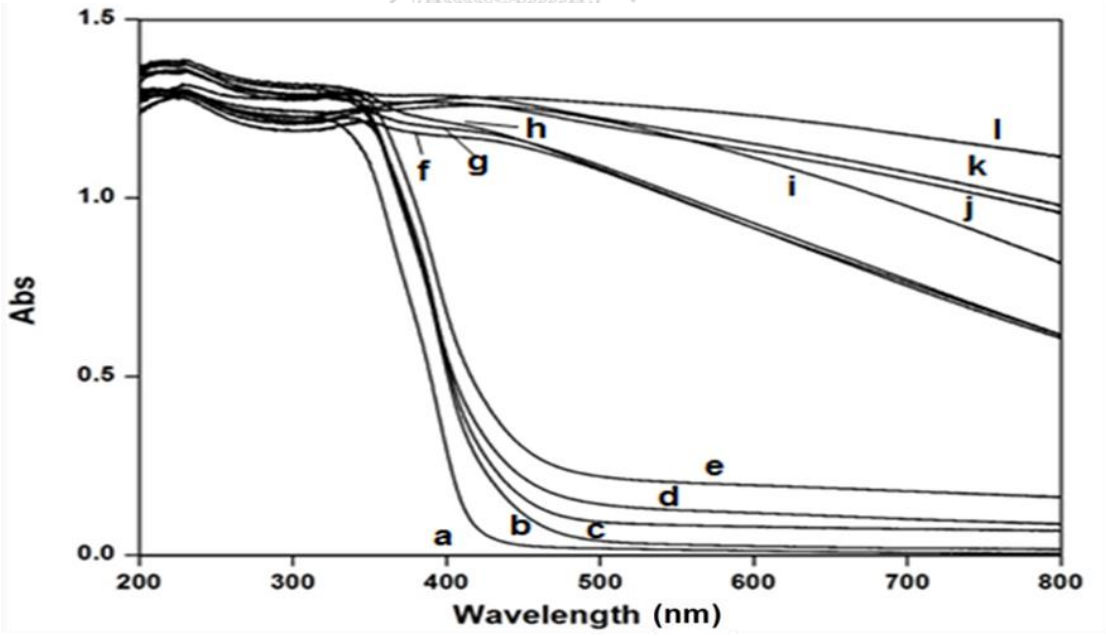

Figure 5.7 UV-vis absorption spectra of (a). TiO_2, (b). 0.5%Ag/TiO_2, (c). 1%Ag/TiO_2, (d). 3%Ag/TiO_2, (e). 2%Ag/TiO_2, (f). 5%PDA-0.5%Ag/TiO_2, (g). 5%PDA-1%Ag/TiO_2, (h). 5%PDA-2%Ag/TiO_2**,** (i). 10%PDA-0.5%Ag/TiO_2, (j). 10%PDA-1%Ag/TiO_2, (k). 10%PDA-3%Ag/TiO_2 and (l). 10%PDA-2%Ag/TiO_2

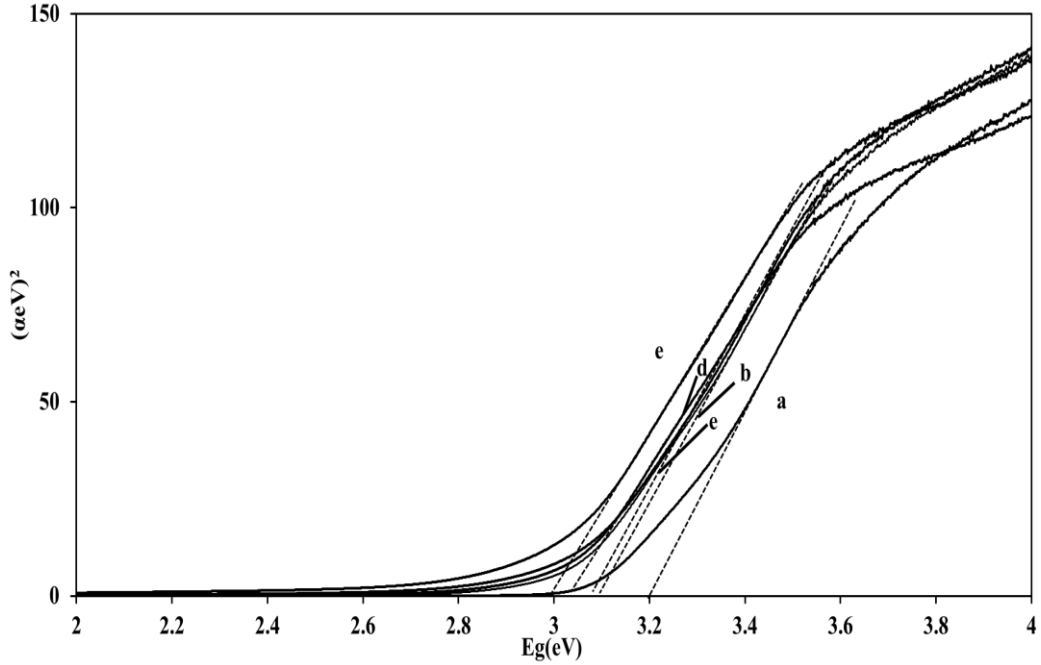

Figure 5.8 Plot of the band gap energy, as derived from the diffuse reflectance UV–Vis spectra for (a). TiO_2, (b). 0.5%Ag/TiO_2, (c). 1%Ag/TiO_2, (d). 3%Ag/TiO_2 and (e). 2%Ag/TiO_2

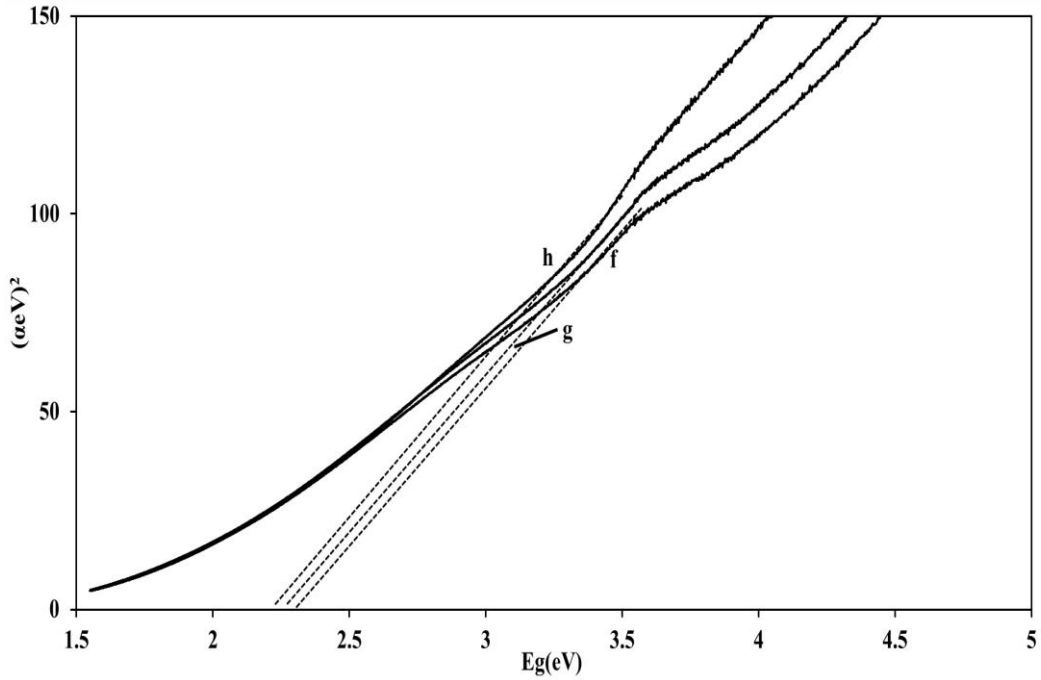

Figure 5.9 Plot of the band gap energy, as derived from the diffuse reflectance UV–Vis spectra for (f). 5%PDA-0.5%Ag/TiO_2, (g). 5%PDA-1%Ag/TiO_2, and (h). 5%PDA-2%Ag/ TiO_2

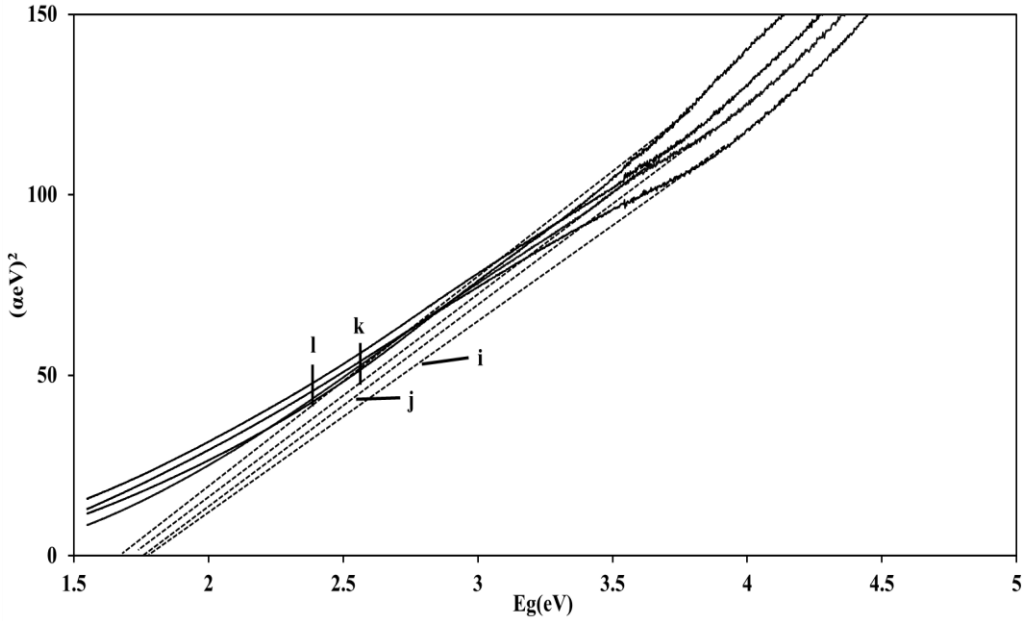

Figure 5.10 Plot of the band gap energy, as derived from the diffuse reflectance UV–Vis spectra for (i). 10%PDA-0.5%Ag/TiO_2, (j). 10%PDA-1%Ag/TiO_2, (k). 10%PDA-3%Ag/TiO_2 and (l). 10%PDA-2%Ag/TiO_2

Table 5.4 The comparison band gap from UV-vis spectra of titanium dioxide doped various amount of Ag and PDA

Sample	Band gap energy (eV)
TiO_2	3.20
0.5%Ag/TiO_2	3.10
1%Ag/TiO_2	3.08
2%Ag/TiO_2	2.99
3%Ag/TiO_2	3.04
5%PDA-0.5%Ag/TiO_2	2.30
10%PDA-0.5%Ag/TiO_2	1.85
5%PDA-1%Ag/TiO_2	2.25
10%PDA-1%Ag/TiO_2	1.80
5%PDA-2%Ag/TiO_2	2.20
10%PDA-2%Ag/TiO_2	1.70
10%PDA-3%Ag/TiO_2	1.76

5.1.8 Photoluminescence measurement

The photoluminescence (PL) spectra were recorded for a study of the optical property of samples, and the experimental results are showed in Figure 5.11-5.13. The PL spectrum of pure TiO_2 displays a strong PL emission at 400-550 nm, related to the highly radiative recombination of photoexcited electrons and holes. Loading Ag on TiO_2 catalysts showed a lower emission intensity due to Ag trapped electron cause the decrease of electron/hole recombination. At 2%wt Ag loading showed the smallest emission peak intensity of various silver. Obviously, the PDA-modified Ag/TiO_2 has a lower emission intensity compared to pure TiO_2 and Ag/TiO_2, and with the increasing PDA amount, the emission intensity gradually weakens which showed a lower photogenerated carrier recombination rate (see figure 5.14). That was, the TiO_2 photogenerated electrons can be effectively transferred to PDA with less charge recombination, which forms more activated OH• for degradation of the MB. This result can be attributed to PDA with semiquinone and quinone functional ligands which act as an electron acceptor [58]. Hence, both the enhanced light absorption and the lowered radiative electron–hole recombination will endow the PDA-Ag/TiO_2 composite with high photocatalytic activity.

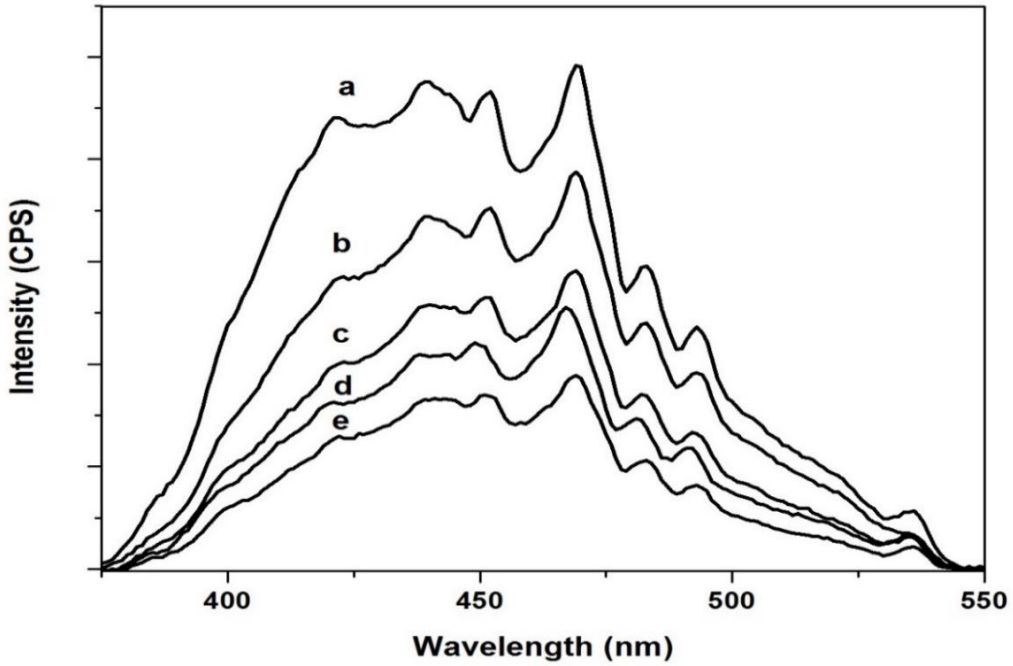

Figure 5.11 Photoluminescence spectra of (a). TiO_2, (b). 0.5%Ag/ TiO_2, (c). 1%Ag/TiO_2, (d). 3%Ag/TiO_2 and (e). 2%Ag/TiO_2 with the excitation wavelength of 325 nm.

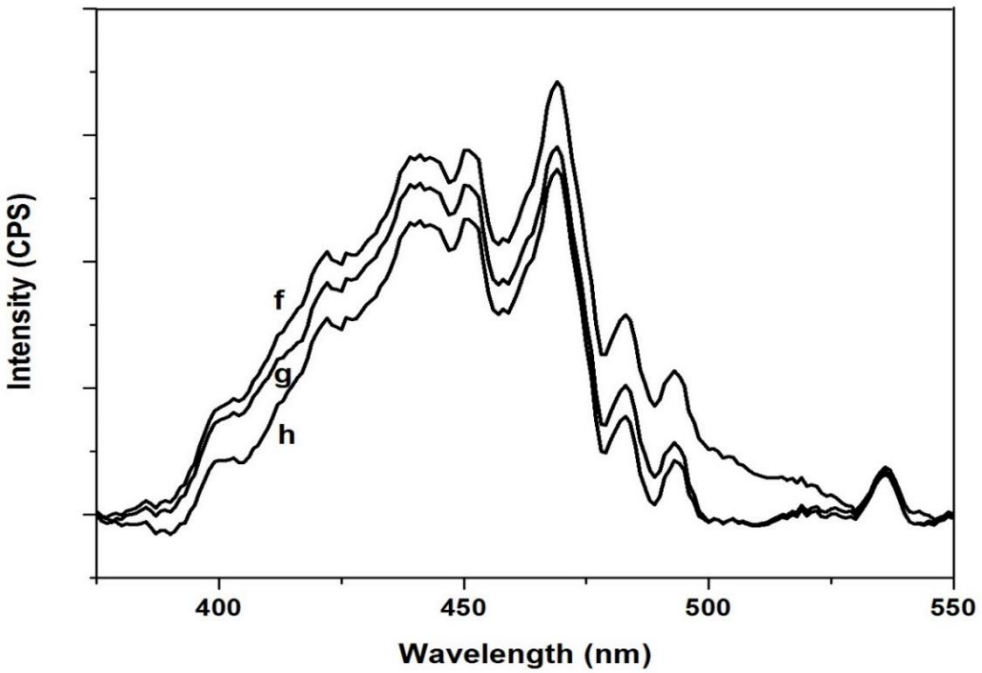

Figure 5.12 Photoluminescence spectra of (f). 5%PDA-0.5%Ag/TiO_2, (g). 5%PDA-1%Ag/TiO_2 and (h). 5%PDA-2%Ag/ TiO_2, with the excitation wavelength of 325 nm

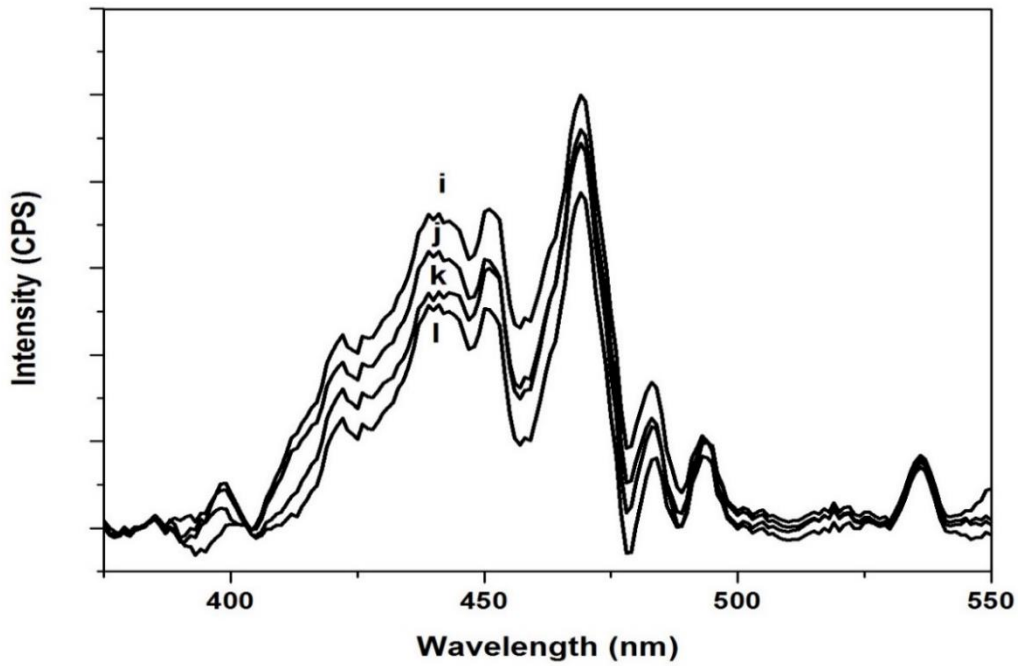

Figure 5.13 Photoluminescence spectra of (i). 10%PDA-0.5%Ag/TiO_2, (j). 10%PDA-1%Ag/TiO_2, (k). 10%PDA-3%Ag/TiO_2 and (l). 10%PDA-2%Ag/TiO_2 with the excitation wavelength of 325 nm

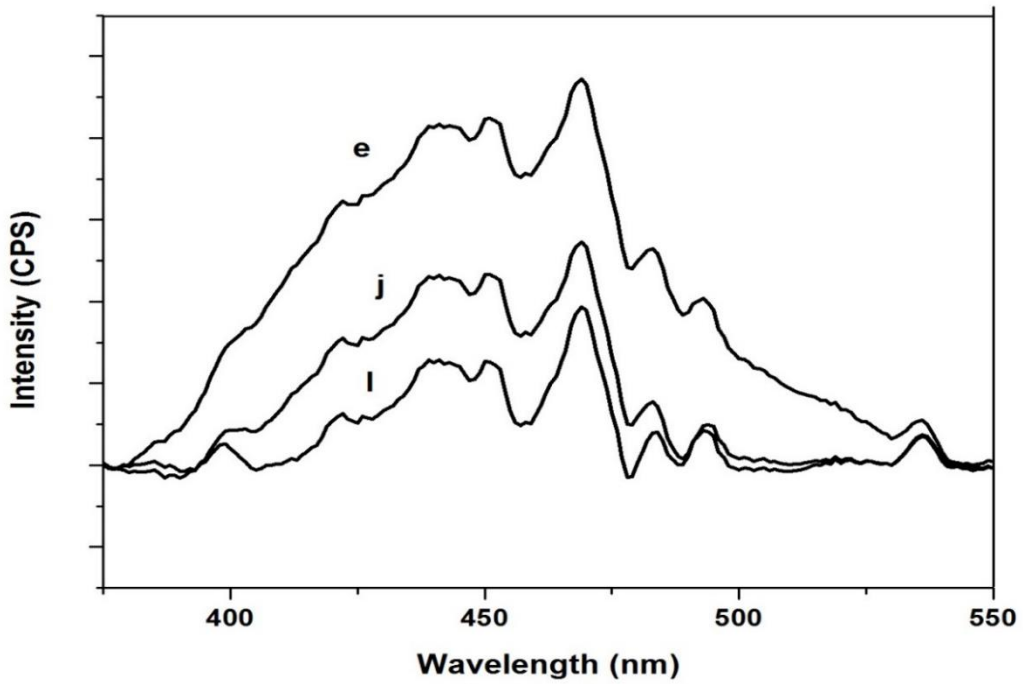

Figure 5.14 Photoluminescence spectra comparison of (e). 2%Ag/TiO_2, (j). 5%PDA-2%Ag/TiO_2 and (l). 10%PDA-2%Ag/TiO_2 with the excitation wavelength of 325 nm

5.2 Photocatalytic activity

The photocatalytic degradation of methylene blue was chosen as a model reaction to evaluate the photocatalytic activities of the catalysts under UV and visible light irradiations. The mixture was stirred in the absence of light for one hour to obtain adsorption equilibrium. After that the mixture was exposed to either UV irradiation or visible light irradiation for 120 minutes. The concentration of methylene blue was measured by UV-visible spectrophotometer.

5.2.1 The catalytic adsorption in the absence of light

Figure 5.15 showed the TiO_2 catalysts adsorbed methylene blue in the absence of light for finding the period of adsorption equilibrium. The result demonstrated that the suitability of adsorption equilibrium was 1 hour due to after 1 hour, the adsorption-desorption remain essential steady.

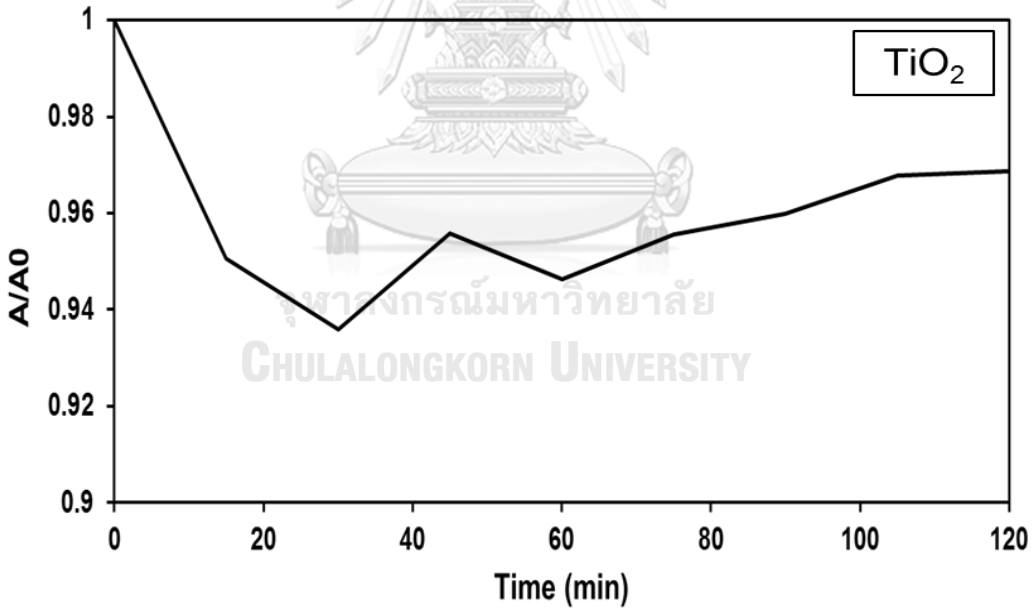

Figure 5.15 catalytic adsorption of methylene blue in the absence of light using TiO_2

5.2.2 The reaction under UV light irradiation

Figure 5.16-5.18 showed the photocatalytic degradation of methylene blue under UV light irradiation, which was used to test the photocatalytic activity.

In figure 5.16 could observe that the photolysis under UV light showed the lowest effect for degradation of methylene blue. The conversion of photolysis was 13.99% (see in table 5.5). The results of methylene blue degradation with catalysts showed that addition of silver exhibited more photocatalytic activity than pure titanium dioxide under UV light. When increasing amount of Ag loading, the degradation of methylene blue increased. The conversion of methylene blue degradation with various Ag loading showed in Table 5.5. This result agreed with the result from photoluminescence measurement. The order of decreasing activity were 2%wt, 3%wt, 1%wt, 0.5%wt and pure TiO_2 and were same as the order of increasing photoluminescence signals (see figure 5.11).

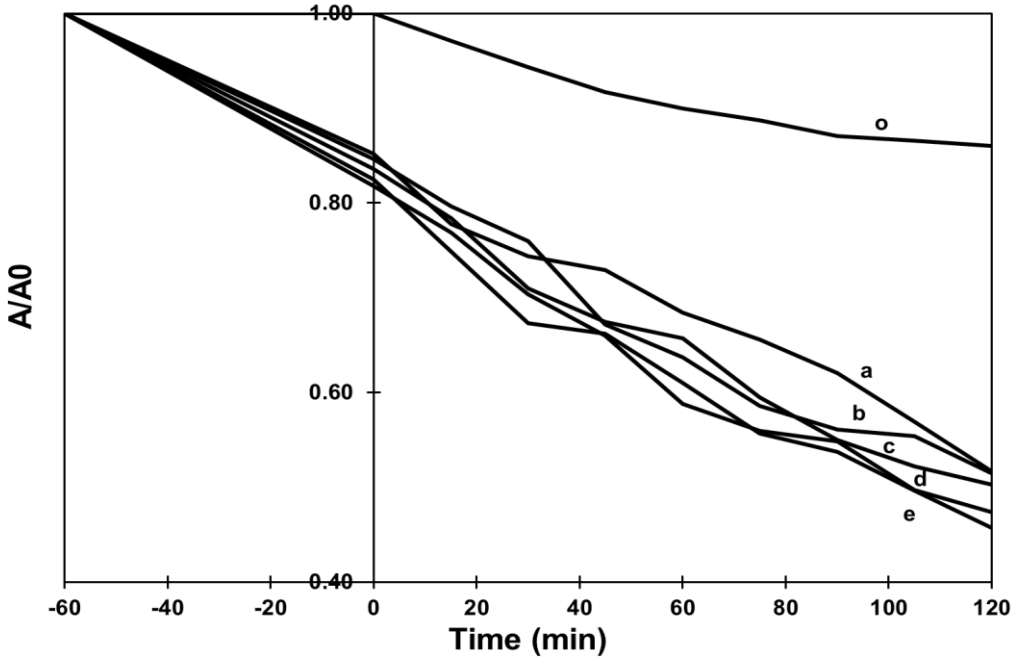

Figure 5.16 Photocatalytic degradation of methylene blue result under UV light irradiations using (o) No catalyst, (a). TiO_2, (b). 0.5%Ag/TiO_2, (c). 1%Ag/TiO_2, (d). 3%Ag/TiO_2 and (e). 2%Ag/TiO_2

Table 5.5 The conversion of methylene blue degradation under UV light using Ag/TiO_2 catalysts

Sample	Conversion (%)
No catalyst	13.99
TiO_2	48.36
0.5%Ag/TiO_2	48.52
1%Ag/TiO_2	49.74
2%Ag/TiO_2	54.27
3%Ag/TiO_2	52.60

In figure 5.17-5.18 showed the 5%wt PDA and 10 %wt modified on Ag/TiO_2, respectively. The results showed that adding PDA on Ag/TiO_2 could increase photocatalytic activity more than pure Ag/TiO_2 and increasing the content of PDA, the photocatalytic activity increased. The photocatalytic degradation depended on the efficient separation of photogenerated charge carriers in titanium dioxide. Therefore, slower recombination of electrons and holes had led to higher photocatalytic activity. As a result, the catalyst with highest activity should produce the smallest signal in photoluminescence measurement (Figures 5.12-5.13). From photoluminescence signal showed PDA-Ag/ TiO_2 had a lower emission intensity than pure TiO_2 and Ag/TiO_2 so PDA could reduce the electron recombination led to high photocatalytic degradation.

At the initial of light irradiation (figure 5.16-5.18) observed that adding PDA on Ag/TiO_2 cause the concentration of methylene blue decreased even absence light because PDA could act like a gripper [44] with a high adsorption efficiency for organic matter which facilitate for methylene blue degradation.

Among the samples, the best performance was attributed to 10%wt PDA-2%wt Ag/TiO_2. This result implied that there was an optimum content of Ag at 2%wt. It could be calculated that the photocatalytic degradation of 10%wt PDA-2%wt Ag/TiO_2 was 87.54% (see in Table 5.6) higher than that of pure titanium dioxide and Ag/TiO_2 catalysts for degradation under UV light because of the lowest electron recombination

and effects of dye adsorption with PDA. Obviously, the photocatalytic activity of PDA-Ag/TiO_2 under UV light demonstrated that Ag and PDA doping effect was outstanding. These agreed with the outcome from the UV-vis spectra and photoluminescence measurement.

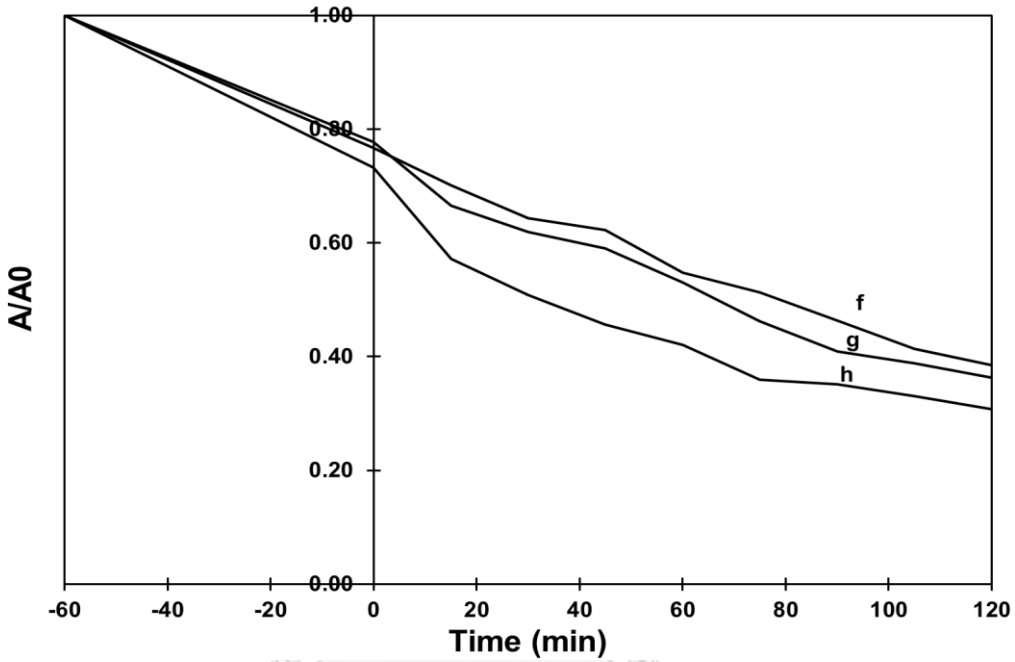

Figure 5.17 Photocatalytic degradation of methylene blue result under UV light irradiations using (f). 5%PDA-0.5%Ag/TiO_2, (g). 5%PDA-1%Ag/TiO_2 and (h). 5%PDA-2%Ag/TiO_2

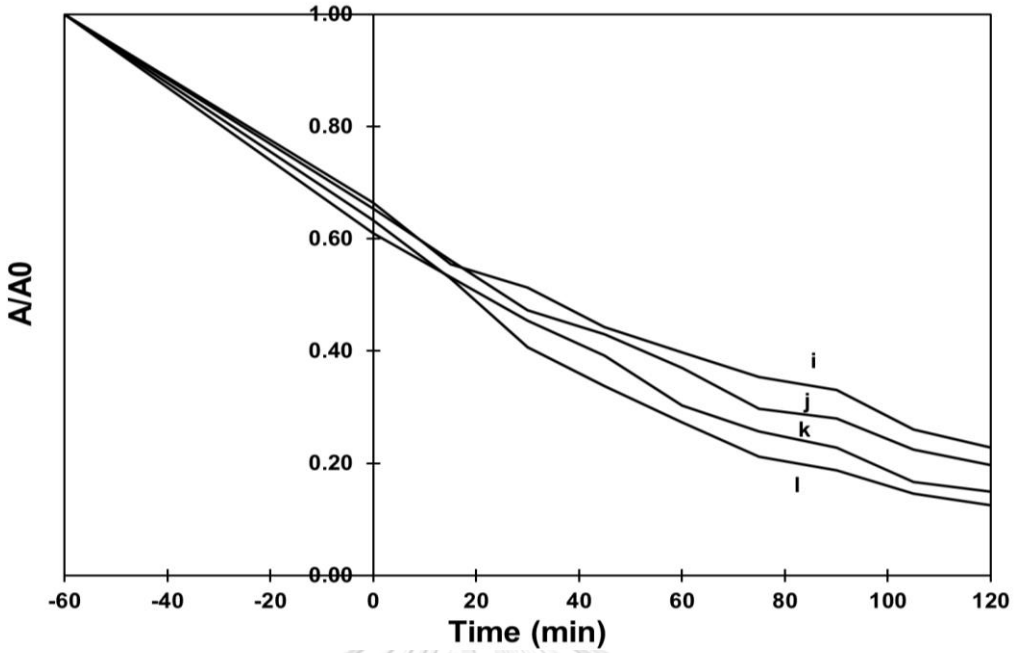

Figure 5.18 Photocatalytic degradation of methylene blue result under UV light irradiations using (i). 10%PDA-0.5%Ag/TiO_2, (j). 10%PDA-1%Ag/TiO_2, (k). 10%PDA-3%Ag/TiO_2 and (l). 10%PDA-2%Ag/TiO_2

Table 5.6 The conversion of methylene blue degradation under UV light using Ag/TiO_2 with 5 or 10 %wt PDA

Sample	Conversion (%)
5%PDA-0.5%Ag/TiO_2	61.56
10%PDA-0.5%Ag/TiO_2	77.21
5%PDA-1%Ag/TiO_2	63.76
10%PDA-1%Ag/TiO_2	80.32
5%PDA-2%Ag/TiO_2	69.28
10%PDA-2%Ag/TiO_2	87.54
10%PDA-3%Ag/TiO_2	86.07

5.2.2 The reaction under visible light irradiation

Figure 5.19-5.21 showed the photocatalytic degradation of methylene blue under visible light irradiation, which was used to test the photocatalytic activity. The photolysis under visible light showed the lowest effect for degradation of methylene blue (in figure 5.19). The conversion of photolysis was 8.29% (see in table 5.5)

In figure 5.19 and Table 5.7 could observe that all amount of silver adding exhibited more photocatalytic activity than pure titanium dioxide under visible light. It could be also see that the addition of silver had an effect on the photodegradation under visible light.

When increasing amount of Ag loading, the degradation of methylene blue increased. This decreasing signal result from photoluminescence measurement was pure TiO_2, 0.5%wt Ag, 1%wt Ag, 3%wt Ag and 2%wt Ag, respectively (see Figure 5.11), as same as the order of increasing absorption spectra (see Figure 5.7) and the order of decreasing the band gap energy (see Figure 5.8 and Table 5.4). Normally in UV-visible light reaction, the mainly characterization method usually analyzed by UV-vis absorption spectra and photoluminescence measurement.

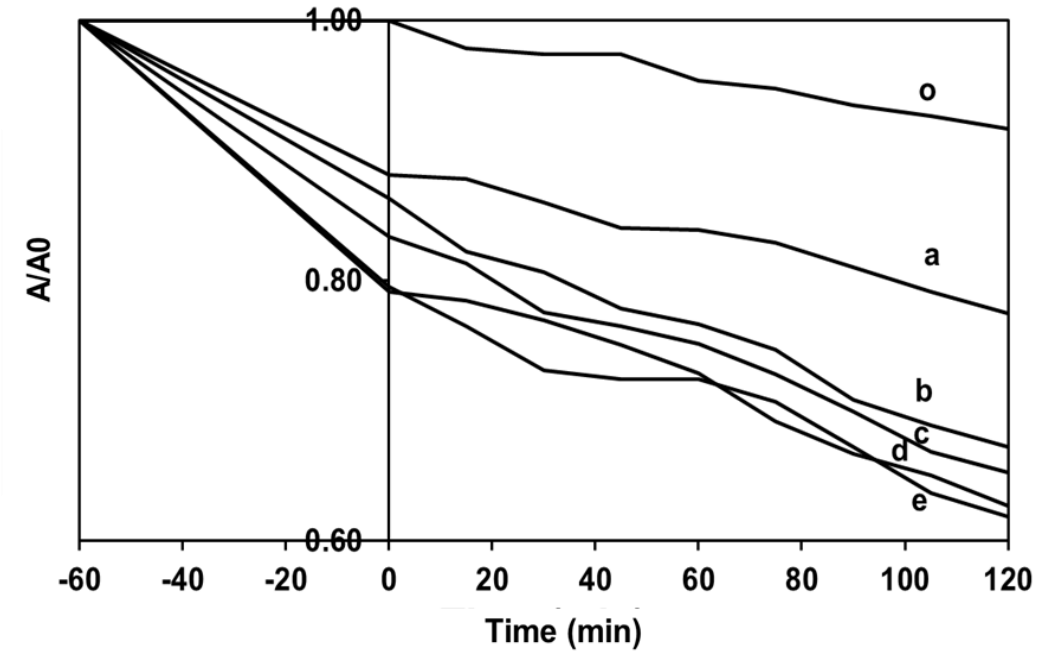

Figure 5.19 Photocatalytic degradation of methylene blue result under Visible light irradiations using (o) No catalyst, (a). TiO_2, (b). 0.5%Ag/ TiO_2, (c). 1%Ag/ TiO_2, (d). 3%Ag/ TiO_2 and (e). 2%Ag/ TiO_2

Table 5.7 The conversion of methylene blue degradation under visible light using Ag/TiO_2 catalysts

Sample	Conversion (%)
No catalyst	8.29
TiO_2	22.53
0.5%Ag/TiO_2	32.73
1%Ag/TiO_2	34.76
2%Ag/TiO_2	38.12
3%Ag/TiO_2	37.80

When doping various PDA on Ag/TiO_2 (see figure 5.20-5.21). The results showed that adding PDA on Ag/TiO_2 could increase photocatalytic activity more than pure Ag/TiO_2 and increasing the content of PDA, the photocatalytic activity increased. From the among characterization result of the catalyst, the best performance should be attributed to 10%PDA-2%Ag/TiO_2 corresponding to the maximum red shift in the UV-vis diffusive reflectance absorption spectra and lowest photoluminescence signal. It could be calculated that the photocatalytic degradation of 2%wt Ag/TiO_2 was 78.98% (see in Table 5.8).

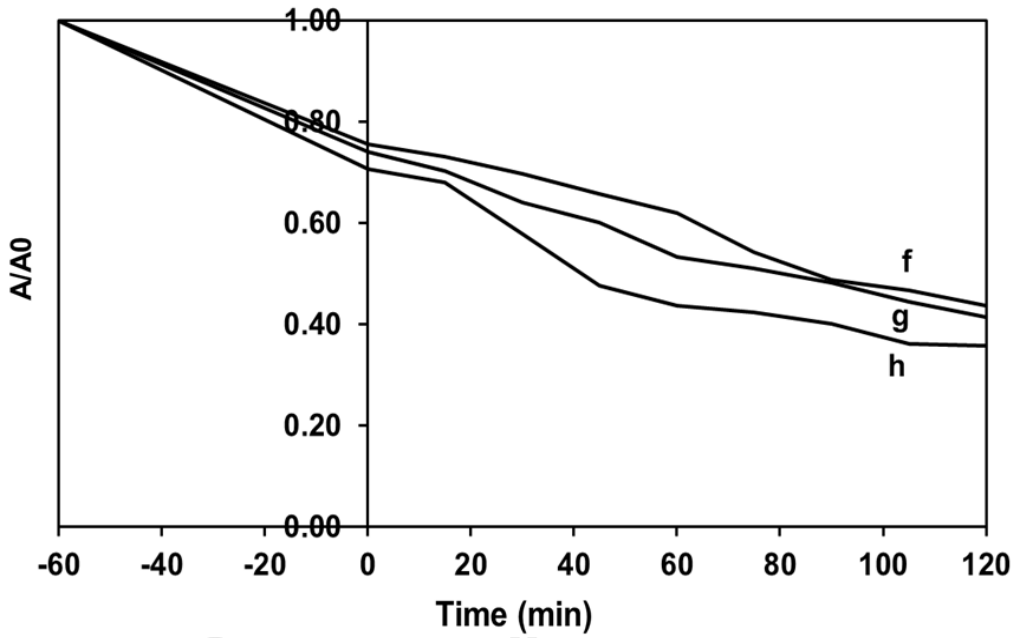

Figure 5.20 Photocatalytic degradation of methylene blue result under Visible light irradiations using (f). 5%PDA-0.5%Ag/TiO_2, (g). 5%PDA-1%Ag/TiO_2 and (h). 5%PDA-2%Ag/TiO_2

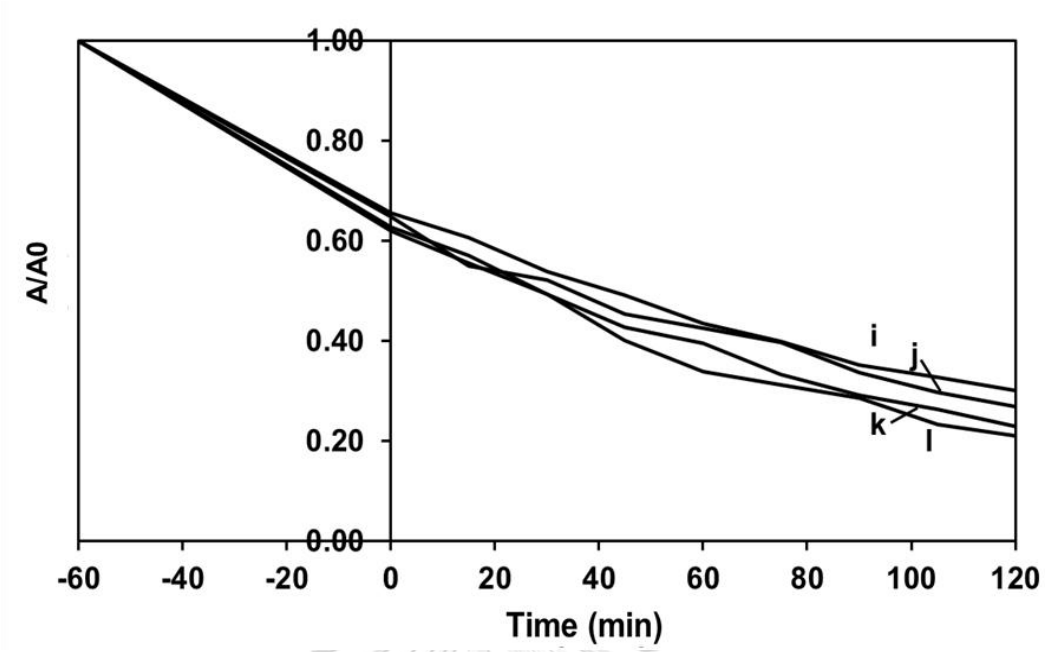

Figure 5.21 Photocatalytic degradation of methylene blue result under Visible light Irradiations using (i). 10%PDA-0.5%Ag/TiO_2, (j). 10%PDA-1%Ag/TiO_2, (k). 10%PDA-3%Ag/TiO_2 and (l). 10%PDA-2%Ag/TiO_2

Table 5.8 The conversion of methylene blue degradation under visible light using Ag/TiO_2 catalysts with 5 or 10 %wt PDA

Sample	Conversion (%)
5%PDA-0.5%Ag/TiO_2	56.18
10%PDA-0.5%Ag/TiO_2	69.75
5%PDA-1%Ag/TiO_2	58.56
10%PDA-1%Ag/TiO_2	73.04
5%PDA-2%Ag/TiO_2	64.12
10%PDA-2%Ag/TiO_2	78.98
10%PDA-3%Ag/TiO_2	76.98

CHAPTER VI

CONCLUSIONS AND RECOMMENDATIONS

In this chapter, section 6.1 provides the conclusions obtained from the experimental results, and the recommendation for further study is also given in section 6.2.

6.1 Conclusions

PDA-Ag/TiO_2 catalysts were successfully prepared by a sol-gel method, followed by impregnation methods. The addition of Ag and especially polydopamine caused the photoluminescence signal smaller and the band gap of the catalyst to become narrower. Therefore, the PDA-Ag/TiO_2 composite was able to absorb light in the visible region. The results of the photodegradation of methylene blue under both UV and visible light confirms that the optimum of Ag loading was 2%wt and 10%PDA-2%Ag/TiO_2 catalyst exhibit highest photocatalytic activity under UV and visible light irradiation. As the amount of PDA was increased, the efficiency of the photocatalytic activity was higher both UV and visible light irradiation because of better absorption in the visible region and slower recombination of photogenerated charge carriers. The PDA-Ag/TiO_2 catalyst not only exhibited superior photocatalytic degradation properties but also possessed excellent adsorption affinity for organic chemicals.

6.2 Recommendations for future studies

1. Investigate the deposition of other metal on the TiO_2 by using incipient wetness impregnation.
2. Variation of PDA loading must be regarded to find optimization configuration.

3. The photocatalytic activity of PDA-Ag/TiO_2 should be investigated in other reaction conditions that catalyst loading, pH value, and the initial dye concentration are varied.

REFERENCES

[1] T. Cattoor, "1 - European legislation relating to textile dyeing A2 - Christie, R.M," in *Environmental Aspects of Textile Dyeing*: Woodhead Publishing, 2007, pp. 1-29.

[2] R. Zallen and M. P. Moret, "The optical absorption edge of brookite TiO2," *Solid State Communications,* Article vol. 137, no. 3, pp. 154-157, 2006.

[3] A. Fujishima and K. Honda, "Electrochemical photolysis of water at a semiconductor electrode," *Nature,* Article vol. 238, no. 5358, pp. 37-38, 1972.

[4] G. Wakefield, M. Green, S. Lipscomb, and B. Flutter, "Modified titania nanomaterials for sunscreen applications - Reducing free radical generation and DNA damage," *Materials Science and Technology,* Conference Paper vol. 20, no. 8, pp. 985-988, 2004.

[5] B. Liu and E. S. Aydil, "Growth of oriented single-crystalline rutile TiO 2 nanorods on transparent conducting substrates for dye-sensitized solar cells," *Journal of the American Chemical Society,* Article vol. 131, no. 11, pp. 3985-3990, 2009.

[6] D. Wodka, R. P. Socha, E. Bielanska, M. Elzbieciak-Wodka, P. Nowak, and P. Warszynski, "Photocatalytic activity of titanium dioxide modified byFe2O3nanoparticles," *Applied Surface Science,* Article vol. 319, no. 1, pp. 173-180, 2014.

[7] Y. Liu, K. Ai, J. Liu, M. Deng, Y. He, and L. Lu, "Dopamine-melanin colloidal nanospheres: An efficient near-infrared photothermal therapeutic agent for in vivo cancer therapy," *Advanced Materials,* Article vol. 25, no. 9, pp. 1353-1359, 2013.

[8] P. Meredith and T. Sarna, "The physical and chemical properties of eumelanin," *Pigment Cell Research,* Review vol. 19, no. 6, pp. 572-594, 2006.

[9] S. Xiong, Y. Wang, J. Yu, L. Chen, J. Zhu, and Z. Hu, "Polydopamine particles for next-generation multifunctional biocomposites," *Journal of Materials Chemistry A,* Article vol. 2, no. 20, pp. 7578-7587, 2014.

[10] W. X. Mao, X. J. Lin, W. Zhang, Z. X. Chi, R. W. Lyu, and A. M. Cao, "Core-shell structured TiO2@polydopamine for highly active visible-light photocatalysis," *Chemical Communications,* Article vol. 52, no. 44, pp. 7122-7125, 2016.

[11] X. Zhou, B. Jin, J. Luo, X. Xu, L. Zhang, and J. Li, "Dramatic visible light photocatalytic degradation due to the synergetic effects of TiO2 and PDA nanospheres," *RSC Advances,* Article vol. 6, no. 69, pp. 64446-64449, 2016.

[12] D. Yang, M. Ruan, S. Huang, Y. Wu, S. Li, and H. Wang, "Improved electromechanical properties of NBR dielectric composites by poly(dopamine) and silane surface functionalized TiO2nanoparticles," *J. Mater. Chem. C,* vol. 4, no. 33, pp. 7724-7734, 2016.

[13] A. Nishimura, G. Mitsui, K. Nakamura, M. Hirota, and E. Hu, "CO 2 reforming characteristics under visible light response of Cr- or Ag-doped TiO 2 prepared by sol-gel and dip-coating process," *International Journal of Photoenergy,* Article vol. 2012, 2012, Art. no. 184169.

[14] L. Yu, J. He, C. Huang, M. Li, Y. Zhang, and X. Zhou, "Electron transportation path build for superior photoelectrochemical performance of Ag3PO4/TiO2," *RSC Advances,* Article vol. 7, no. 86, pp. 54485-54490, 2017.

[15] J. N. Schrauben, R. Hayoun, C. N. Valdez, M. Braten, L. Fridley, and J. M. Mayer, "Titanium and zinc oxide nanoparticles are proton-coupled electron transfer agents," *Science,* Article vol. 336, no. 6086, pp. 1298-1301, 2012.

[16] U. Diebold, "The surface science of titanium dioxide," *Surface Science Reports,* vol. 48, no. 5, pp. 53-229, 2003/01/01/ 2003.

[17] A. Fujishima and X. Zhang, "Titanium dioxide photocatalysis: present situation and future approaches," *Comptes Rendus Chimie,* vol. 9, no. 5, pp. 750-760, 2006/05/01/ 2006.

[18] A. Fujishima, X. Zhang, and D. A. Tryk, "TiO2 photocatalysis and related surface phenomena," *Surface Science Reports,* vol. 63, no. 12, pp. 515-582, 2008/12/15/ 2008.

[19] A. Sclafani and J. M. Herrmann, "Comparison of the photoelectronic and photocatalytic activities of various anatase and rutile forms of titania in pure

liquid organic phases and in aqueous solutions," *Journal of Physical Chemistry,* Article vol. 100, no. 32, pp. 13655-13661, 1996.

[20] X. Chen, "Titanium Dioxide Nanomaterials and Their Energy Applications," *Chinese Journal of Catalysis,* vol. 30, no. 8, pp. 839-851, 2009/08/01/ 2009.

[21] D. Regonini, C. R. Bowen, A. Jaroenworaluck, and R. Stevens, "A review of growth mechanism, structure and crystallinity of anodized TiO2 nanotubes," *Materials Science and Engineering: R: Reports,* vol. 74, no. 12, pp. 377-406, 2013/12/01/ 2013.

[22] Y.-F. Chen, C.-Y. Lee, M.-Y. Yeng, and H.-T. Chiu, "The effect of calcination temperature on the crystallinity of TiO2 nanopowders," *Journal of Crystal Growth,* vol. 247, no. 3, pp. 363-370, 2003/01/01/ 2003.

[23] L. L. Hench and J. K. West, "The sol-gel process," *Chemical Reviews,* vol. 90, no. 1, pp. 33-72, 1990/01/01 1990.

[24] J.-M. Herrmann, "Fundamentals and misconceptions in photocatalysis," *Journal of Photochemistry and Photobiology A: Chemistry,* vol. 216, no. 2, pp. 85-93, 2010/12/15/ 2010.

[25] "IFC Editorial Board," *Applied Catalysis B: Environmental,* vol. 70, no. 1, p. CO2, 2007/01/31/ 2007.

[26] M.-H. Weng, C. Chen, and S.-P. Ju, "A First-Principle Study on Size-Dependent Thermodynamic Properties of Small TiO2 Nanoclusters," *Chinese Journal of Catalysis,* vol. 30, no. 5, pp. 384-390, 2009/05/01/ 2009.

[27] X. Chen and S. S. Mao, "Titanium dioxide nanomaterials: Synthesis, properties, modifications and applications," *Chemical Reviews,* Review vol. 107, no. 7, pp. 2891-2959, 2007.

[28] U. G. Akpan and B. H. Hameed, "Parameters affecting the photocatalytic degradation of dyes using TiO2-based photocatalysts: A review," *Journal of Hazardous Materials,* vol. 170, no. 2, pp. 520-529, 2009/10/30/ 2009.

[29] I. K. Konstantinou and T. A. Albanis, "TiO2-assisted photocatalytic degradation of azo dyes in aqueous solution: Kinetic and mechanistic investigations: A review," *Applied Catalysis B: Environmental,* Article vol. 49, no. 1, pp. 1-14, 2004.

[30] W.-T. Chang, Y.-C. Hsueh, S.-H. Huang, K.-I. Liu, C.-C. Kei, and T.-P. Perng, "Fabrication of Ag-loaded multi-walled TiO2 nanotube arrays and their photocatalytic activity," *Journal of Materials Chemistry A,* 10.1039/C2TA00806H vol. 1, no. 6, pp. 1987-1991, 2013.

[31] L. Ge, M. Xu, and H. Fang, "Preparation and characterization of silver and indium vanadate co-doped TiO2 thin films as visible-light-activated photocatalyst," *Journal of Sol-Gel Science and Technology,* journal article vol. 40, no. 1, pp. 65-73, October 01 2006.

[32] H. Li, X. Duan, G. Liu, and X. Liu, "Photochemical synthesis and characterization of Ag/TiO2 nanotube composites," *Journal of Materials Science,* journal article vol. 43, no. 5, pp. 1669-1676, March 01 2008.

[33] H. Lee, S. M. Dellatore, W. M. Miller, and P. B. Messersmith, "Mussel-inspired surface chemistry for multifunctional coatings," *Science,* Article vol. 318, no. 5849, pp. 426-430, 2007.

[34] Y. Liu, K. Ai, and L. Lu, "Polydopamine and its derivative materials: Synthesis and promising applications in energy, environmental, and biomedical fields," *Chemical Reviews,* Review vol. 114, no. 9, pp. 5057-5115, 2014.

[35] N. Liu, S. Chen, Y. Li, H. Dai, and Y. Lin, "Self-enhanced photocathodic matrix based on poly-dopamine sensitized TiO2 mesocrystals for mycotoxin detection assisted by a dual amplificatory nanotag," *New Journal of Chemistry,* Article vol. 41, no. 9, pp. 3380-3386, 2017.

[36] A. Postma, Y. Yan, Y. Wang, A. N. Zelikin, E. Tjipto, and F. Caruso, "Self-polymerization of dopamine as a versatile and robust technique to prepare polymer capsules," *Chemistry of Materials,* Article vol. 21, no. 14, pp. 3042-3044, 2009.

[37] A. B. Mostert *et al.*, "Role of semiconductivity and ion transport in the electrical conduction of melanin," *Proceedings of the National Academy of Sciences of the United States of America,* Article vol. 109, no. 23, pp. 8943-8947, 2012.

[38] M. Vaselbehagh, H. Karkhanechi, S. Mulyati, R. Takagi, and H. Matsuyama, "Improved antifouling of anion-exchange membrane by polydopamine coating

in electrodialysis process," *Desalination,* vol. 332, no. 1, pp. 126-133, 2014/01/02/ 2014.

[39] Y. A. M. Akl Ma, "Solid Phase Extraction and Spectrophotometric Determination of Methylene Blue in Environmental Samples using Bentonite and Acid Activated Bentonite from Egypt," *Journal of Analytical & Bioanalytical Techniques,* vol. 05, no. 01, 2014.

[40] L. Jiang, G. Zhou, J. Mi, and Z. Wu, "Fabrication of visible-light-driven one-dimensional anatase TiO2/Ag heterojunction plasmonic photocatalyst," *Catalysis Communications,* vol. 24, pp. 48-51, 2012/07/05/ 2012.

[41] D.-S. Lee and Y.-W. Chen, "Nano Ag/TiO2 catalyst prepared by chemical deposition and its photocatalytic activity," *Journal of the Taiwan Institute of Chemical Engineers,* vol. 45, no. 2, pp. 705-712, 2014/03/01/ 2014.

[42] J. Kong, C. Song, W. Zhang, Y. Xiong, M. Wan, and Y. Wang, "Enhanced visible-light-active photocatalytic performances on Ag nanoparticles sensitized TiO2 nanotube arrays," *Superlattices and Microstructures,* vol. 109, pp. 579-587, 2017/09/01/ 2017.

[43] G. Dawson, J. Liu, L. Lu, and W. Chen, "Dopamine-Modified Trititanate Nanotubes with UV- and Visible-Light Photocatalytic Activity: Coordinative Self-Assembly into a Recyclable Absorber," *ChemCatChem,* Article vol. 4, no. 8, pp. 1133-1138, 2012.

[44] H. Wang, F. Jiang, Y. Zhu, and Y. Zhao, "Photocatalytic properties of polydopamine-modified Ag NP/TiO2 porous nanofibers prepared by electrospinning," *RSC Advances,* Article vol. 5, no. 126, pp. 104314-104321, 2015.

[45] S. Kim, G. H. Moon, G. Kim, U. Kang, H. Park, and W. Choi, "TiO2 complexed with dopamine-derived polymers and the visible light photocatalytic activities for water pollutants," *Journal of Catalysis,* Article vol. 346, pp. 92-100, 2017.

[46] Z. Yu, F. Li, Q. Yang, H. Shi, Q. Chen, and M. Xu, "Nature-Mimic Method to Fabricate Polydopamine/Graphitic Carbon Nitride for Enhancing Photocatalytic Degradation Performance," *ACS Sustainable Chemistry and Engineering,* Article vol. 5, no. 9, pp. 7840-7850, 2017.

[47] G. Loget, J. E. Yoo, A. Mazare, L. Wang, and P. Schmuki, "Highly controlled coating of biomimetic polydopamine in TiO2 nanotubes," *Electrochemistry Communications,* vol. 52, pp. 41-44, 2015.

[48] J. C. M. E. Res, *Nanostructured TiO2 Obtained by Electrolysis and its Application in the Remediation of Water Polluted with Paracetamol*. 2016, pp. 20-28.

[49] R. Nirmala, J. Jin Won, R. Navamathavan, and K. Hak Yong, "Synthesis and electrical properties of TiO2 nanoparticles embedded in polyamide-6 nanofibers via electrospinning," *Nano-Micro Letters,* vol. 3, no. 1, pp. 56-61, 2011-05-13 2011.

[50] E. L. L. K. F. W. T. S. X. H. Y. Y. H. L. J. Fan, "Photocatalytic Reduction ofCO2 into Methanol over Ag/TiO2 Nanocomposites Enhanced by Surface Plasmon Resonance," *Plasmonics,* pp. 61-70, 2013.

[51] Y. J. Kim, H. J. Kwon, I.-S. Nam, J. W. Choung, J. K. Kil, and H.-J. Kim, "High deNOx performance of Mn/TiO2 catalyst by NH3," *Catalysis Today,* vol. 151, no. 3, pp. 244-250, 2010/06/19/ 2010.

[52] P. Zhang, T. Song, T. Wang, and H. Zeng, "Enhancement of hydrogen production of a Cu–TiO2 nanocomposite photocatalyst combined with broad spectrum absorption sensitizer Erythrosin B," *RSC Advances,* vol. 7, no. 29, pp. 17873-17881, 2017.

[53] M. Rahmati *et al.*, "Effects of Ag promotion and preparation method on cobalt Fischer-Tropsch catalysts supported on silica-modified alumina," *Journal of Catalysis,* vol. 362, pp. 118-128, 2018.

[54] E. Filippo, C. Carlucci, A. L. Capodilupo, P. Perulli, F. Conciauro, and G. A. Corrente, "Enhanced Photocatalytic Activity of Pure Anatase Tio2 and Pt-Tio2 Nanoparticles Synthesized by Green Microwave Assisted Route," *Materials Research,* vol. 18, no. 3, pp. 473-481, 2015.

[55] C. Martín, V. Rives, V. Sánchez-Escribano, G. Busca, V. Lorenzelli, and G. Ramis, "Surface reactivity and morphology of vanadia-titania catalysts," *Surface Science,* vol. 251-252, pp. 825-830, 1991/07/01/ 1991.

[56] K. Chen, K. Xie, Q. Long, L. Deng, Z. Fu, and H. Xiao, "Fabrication of core–shell Ag@pDA@HAp nanoparticles with the ability for controlled release of Ag+ and

superior hemocompatibility," *RSC Advances,* vol. 7, no. 47, pp. 29368-29377, 2017.

[57] S. Kim, G.-h. Moon, G. Kim, U. Kang, H. Park, and W. Choi, "TiO2 complexed with dopamine-derived polymers and the visible light photocatalytic activities for water pollutants," *Journal of Catalysis,* vol. 346, pp. 92-100, 2017.

[58] S. Krejčíková, L. Matějová, K. Kočí, L. Obalová, Z. Matěj, and L. Čapek, "Preparation and characterization of Ag-doped crystalline titania for photocatalysis applications," *Applied Catalysis B: Environmental,* vol. 111-112, pp. 119-125, 2012/01/12/ 2012.

APPENDIX

APPENDIX A

CALCULATION OF CATALYST PREPARATION

Preparation of Ag/TiO_2 by incipient wetness impregnation method

Reagents:

TiO_2 powder was prepared by a sol-gel method.

Silver nitrate >99.999%, $AgNO_3$ (Aldrich Chemical)

Calculation for preparation of Ag/TiO_2 catalysts

To determine the catalyst composition (for example, 2%Ag/ TiO_2)

Basis: 1g of catalyst

Ag = 0.02 x 1 = 0.02 g

TiO_2 = 1-0.02 = 0.08 g

Ag 0.02 g was prepared from $AgNO_3$ as precursor of silver

$$\mathrm{AgNO_3\,used} = \frac{\mathrm{Ag\ required}}{\mathrm{MW\ of\ Ag}} \times \mathrm{MW\ of\ AgNO_3}$$

$$= \frac{0.02\ \mathrm{g}}{107.87\ \mathrm{g/mol}} \times 169.87\ \mathrm{g/mol}$$

$$= 0.0315\ \mathrm{g}$$

Note: Molecular weight of $AgNO_3$ equal to 169.87 g/mole

Molecular weight of Ag equal to 107.87 g/mole

Preparation of PDA-Ag/TiO_2 catalysts

Reagents:

Ag/TiO_2 powder was prepared by incipient wetness impregnation method.

Dopamine hydrochloride, $C_8H_{11}NO_2 \cdot HCl$ (Aldrich chemical)

Calculation for preparation of PDA-Ag/TiO_2 catalysts

To determine the catalyst composition (for example, 5%PDA-2%Ag/TiO_2)

Basis: 1g of catalyst

DA = 0.05 * 1 = 0.05 g

Ag/TiO_2 = 1-0.05 = 0.95 g

DA 0.05 g was prepared from $C_8H_{11}NO_2$·HCl as precursor

$$\mathrm{C_8H_{11}NO_2HCl} = \frac{\textbf{DA required}}{\textbf{MW of DA}} \text{ x MW of } \mathrm{C_8H_{11}NO_2HCl}$$

$$= \frac{0.05\ \mathrm{g}}{153.18\ \mathrm{g/mol}} \text{ x } 189.64\ \mathrm{g/mol}$$

$$= 0.062\ \mathrm{g}$$

Note: Molecular weight of $C_8H_{11}NO_2$·HCl equal to 189.64 g/mole

Molecular weight of DA equal to 153.18 g/mole

APPENDIX B

LIGHTING INSTRUMENT

Intensity of both light bulbs was measured by light sensor (IL 1700 research radiometer) of both UV and visible range, as showed in Table B.1.

Table B.1 The light bulb properties of using the photocatalytic activity

Type of light bulb	Type of light	Power (W)	Intensity by sensor UV light (%)	Intensity by sensor visible light (%)
(Philips)	UV light (253 nm)	75	99.69	0.31
Daylight (Philips)	Visible light (400-700 nm)	18	1.01	98.99

APPENDIX C

CALCULATION OF THE CRYSTALLITE SIZE

Calculation of the crystallite size by Debye-Scherrer equation.

The crystallite size was calculated from the width at half-height of the diffraction peak of XRD pattern using the Debye-Scherrer equation.

From Scherrer equation:

$$D = \frac{K\lambda}{\beta\cos\theta} \qquad (B1)$$

Where D = Crystallite size, A

K = Crystallite shape factor = 0.9

λ = X-ray wavelength, 1.5418 Å for Cu$K\alpha$

θ = Observed peak angle, degree

β = X-ray diffraction broadening, radian

The X-ray diffraction broadening (β) is the corrected width of power diffraction free from all broadening due to the instrument. The α-Alumina was used as a standard sample to provide instrumental broadening data (see Figure B.2). The most common correction for the X-ray diffraction broadening (β) can be obtained by using the Warren formula.

From Warren's formula:

$$\beta = \sqrt{B_m^2 - B_s^2} \qquad (C2)$$

Where B_M = The measured peak width in radians at half peak height.

B_S = The corresponding width of a standard material.

Example: Calculation of the crystallite size of TiO_2

From Figure C.1**,** the 101 diffraction peak of TiO_2 for calculation of crystallite size

An interesting diffraction peak is the plane occurred at the 2θ of 25.24^o

The half-height width of diffraction peak = 0.92^{o}

= (2π x 0.92)/360

=0.0161 radian

The corresponding half-height width of peak of α-alumina = 0.004 radian

The broadening $\beta = \sqrt{B_m^2 - B_s^2}$,

$$= \sqrt{0.0161^2 - 0.004^2}$$

$$\beta = 0.01568 \text{ radian}$$

$$2\theta = 25.24\,^{\circ}$$

$$\theta = 12.62\,^{\circ}$$

$$\lambda = 1.5418 \text{ Å}$$

The crystallite size $= \frac{0.9x1.5418}{0.01568xcos(12.62)} = 88.60$ Å

$$= 8.86 \text{ nm}$$

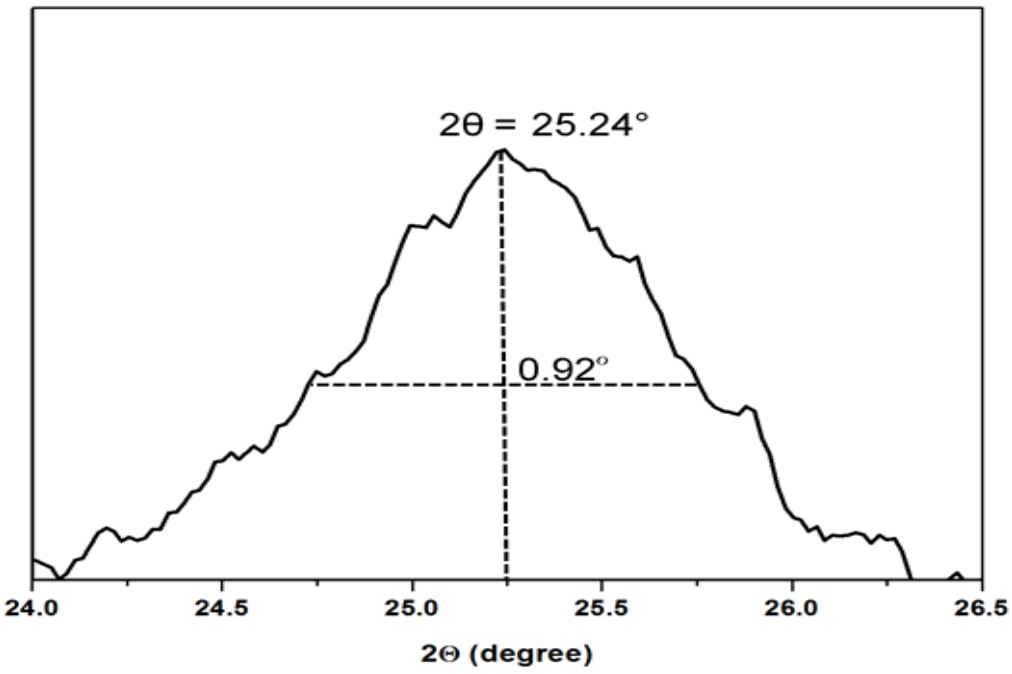

Figure C.1 The 101 diffraction peak of TiO_2 for calculation of the crystallite size

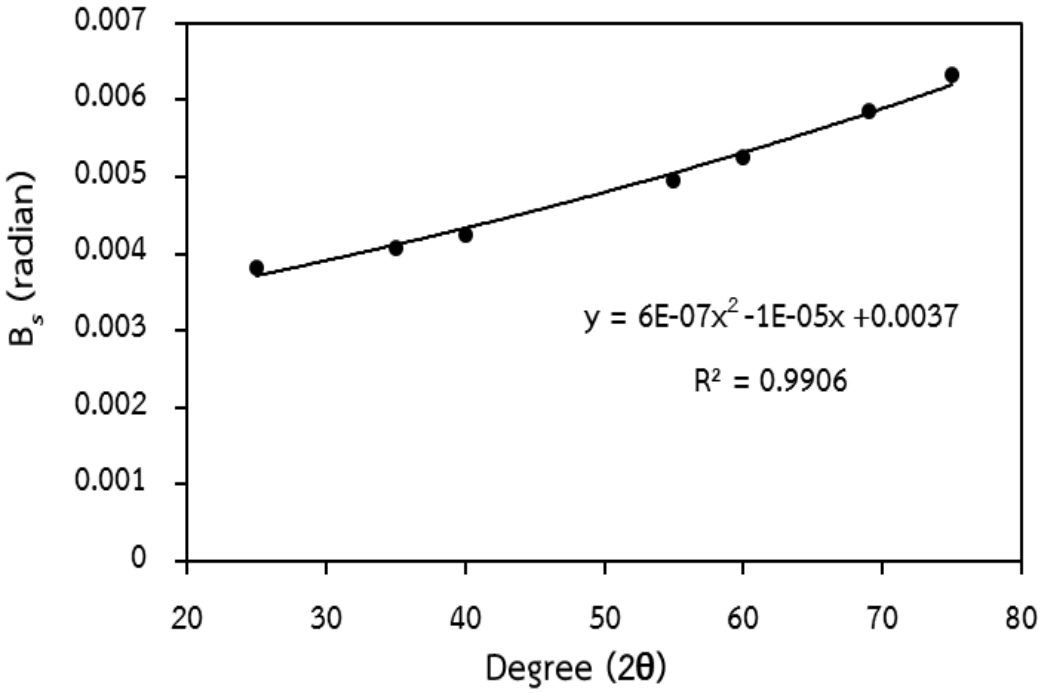

Figure C.2 The plot indicating the value of line broadening due to the equipment. The data were obtained by using α-alumina as standard

APPENDIX D

CALIBRATION CURVE OF METHYLENE BLUE

This appendix showed the calibration curves for calculation concentration of methylene blue in Photocatalytic degradation of methylene blue reaction.

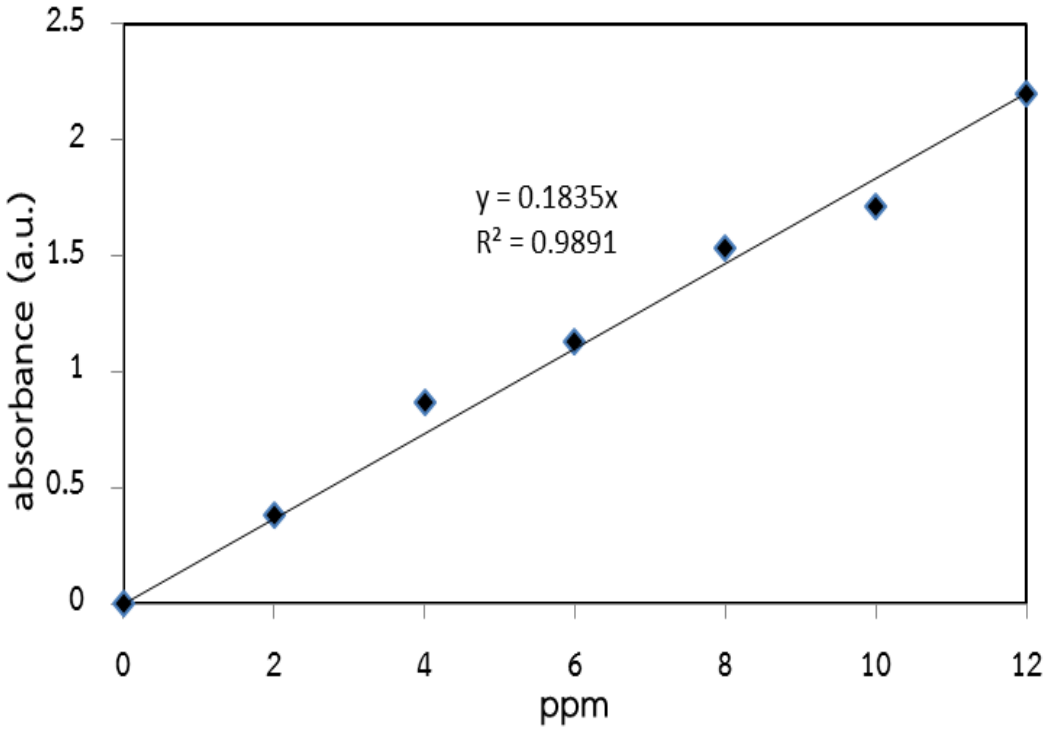

Figure D.1 The calibration cure of methylene blue from UV-Vis scanning spectrophotometer Perkin – Elmer lambda 650

APPENDIX E

CALCULATION OF RESULT OF ICP-OES

Calculation of ICP-OES

The results from ICP-OES characterization were calculation the contents of metal in catalysts. The example of calculation is following:

Example: calculation of the contents of 0.5% of Ag/TiO_2

For 0.5% of Ag/TiO_2, the initial weight of powder was 0.12 g

Hence, the calculation of silver contents as follows:

The amount of silver in catalyst were:

In 100 g of the of the Ag/TiO_2 had a Ag content was 0.5 g

In 0.12 g of the of the Ag/TiO_2 had a Ag content was $\frac{0.5 \times 0.12}{100}$

= 0.6 mg

For digestion, the samples were diluted to 100 ml

Thus;

The concentration of the sample was $\frac{0.6 \times 1000}{100}$ = 6 ppm of Ag

From the result of ICP-OES, The concentration of Ag was 4.39 ppm

Thus;

The Ag contents of Ag/TiO_2 catalyst were:

The Ag concentration was 6 ppm refer to 0.5 %wt Ag/TiO_2

The Ag concentration was 4.39 ppm refer to $\frac{4.39 \times 0.5}{6}$

= 0.37 %wt of Ag/TiO_2

APPENDIX F

CALCULATION OF CO CHEMISORPTION

The silver metal dispersion measured by CO adsorption and calculations were follows by

Calculation of the silver active site

$$\text{Ag active site} = S_f \times \frac{V_{ads}}{V_g} \times N_A \qquad \text{(F1)}$$

Where S_f = stoichiometry factor, (CO : Ag = 1)

V_{ads} = volume of chemisorbed (cm^3/g)

V_g = molar volume of gas at STP = 22,414 (cm^3/mol)

N_A = Avogadro's number = 6.023×10^{23}

Calculation of the silver metal dispersion

Metal dispersion (%) = $100 \times \frac{\text{molecule of Ag from CO adsorption}}{\text{molecule of Ag loaded}}$

Thus, the formula of metal dispersion

$$\%D = S_f \times \frac{V_{ads}}{V_g} \times \frac{M.W.}{\%M} \times 100\% \times 100\% \qquad \text{(F2)}$$

Where %D = % Ag metal dispersion

S_f = stoichiometry factor, (CO : Ag = 1)

V_{ads}= volume of chemisorbed (cm^3/g)

V_g= molar volume of gas at STP = 22,414 (cm^3/mol)

M.W. = molecular weight of silver (a.m.u.)

%M = weight percent silver loading

Calculation of Volume chemisorbed

$$V_{ads} = \frac{V_{inj}}{M} \text{ x } \sum_{i=1}^{n}(1 - \frac{A_i}{A_f}) \qquad (F3)$$

Where V_{ads}= volume of chemisorbed (cm^3/g)

V_{inj} = volume injected = 0.02 cm^3

M = mass of catalyst sample (g)

A_f = area of peak last peak

A_i = area of peak i

i = start at this value

n = go to this value

For example: 0.5%Ag/TiO_2

Where V_{inj} = 20 µl

M = 0.0522 g

i = 1

n = 4

No. peak	A_i	$\frac{A_i}{A_f}$	$1 - \frac{A_i}{A_f}$
1	0.044	0.96	0.043
2	0.045	0.97	0.034
3	0.046	0.99	0.011
4	0.046	1	0
Sum			0.088

Thus, $\sum_{i=1}^{4}(1-\frac{A_i}{A_f})$ = 0.088

Replaced the values into equation (1), (2) and (3)

Eq. (F3)

$$V_{ads} = \frac{0.02}{0.0522} \text{ x } 0.088$$

$$V_{ads} = 0.035 \text{ cm}^3$$

Eq. (F1)

$$\text{Ag active site} = 1\text{x}\frac{0.035}{22{,}414} \text{ x } 6.023 \text{ x } 10^{23}$$

$$\text{Ag active site} = 9.40\text{x}10^{17} \; molecule\; CO/g$$

Eq. (F2)

$$\%D = 1\text{x}\frac{0.035}{22{,}414} \text{ x } \frac{107.87}{0.37} \text{ x } 100\% \text{ x } 100\%$$

$$\%D = 4.55\ \%$$

APPENDIX G

CALCULATION OF AMOUNT OF POLYDOPAMINE

The amount of polydopamine on titanium dioxide was determined by UV-visible absorption spectroscopy.

The standard of polydopamine was prepared by adding 100 mL of tris-buffer solution (10 mM) was added to 100 mL of DI water.The mixture was stirred at a room temperature for 15 minutes. After that, dopamine hydrochloride (i.e., to obtain 70 ppm) were added to 100 mL of DI water and the pH of the mixture solution was adjusted to 8.5 using NaOH solution. The mixture was stirred at a room temperature for 30 minutes.

The calibration curve of the concentration of polydopamine with absorbance was illustrated in the following figure.

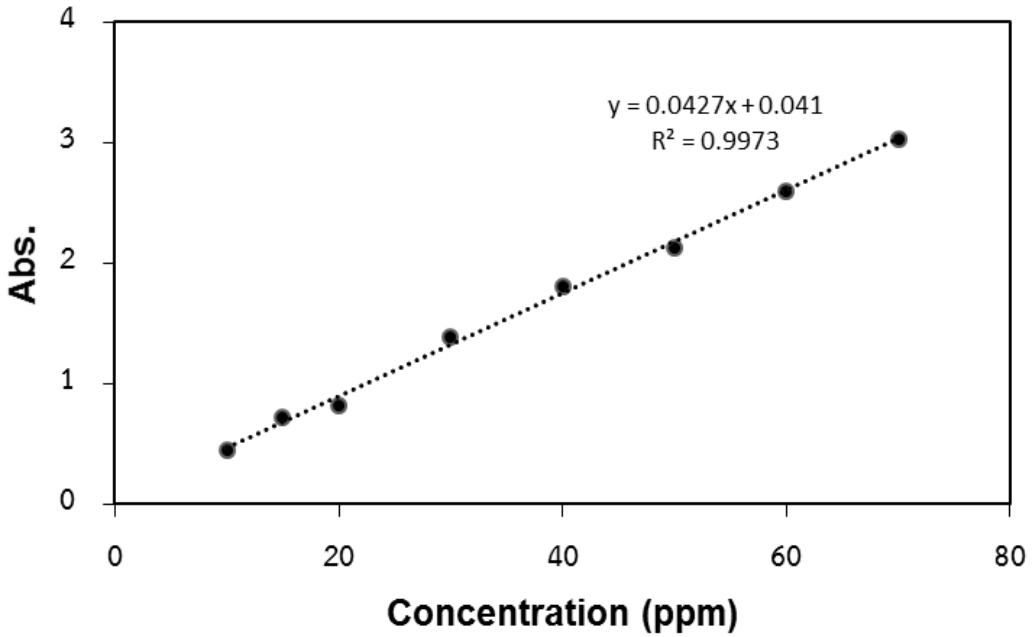

Figure G.1 The calibration curve of the concentrate of polydopamine at the Wavelength of 280 nm

APPENDIX H

THE CALCULATION OF THE BAND GAP FROM UV-VIS SPECTRA

The band gap (E_g) of the sample was determined by the following equation:

$$E_g = \frac{hC}{\lambda} \qquad (H.1)$$

and

$$(\alpha eV)^2 = (\ln\left(\frac{10^{(2-A)}}{100}\right) x E_g)^2 \qquad (H.1)$$

Where E_g = band gap (eV)

h = Planks constant = 6.63×10^{-34} Joules sec

C = Speed of light = 3.0×10^{8} meter/sec

λ = Cut off wavelength (meters)

α = The absorption coefficient in cm^{-1}

A = Absorbance

1eV = 1.6×10^{-19} Joules (conversion factor)

Plot $(\alpha eV)^2$ against E_g and the extrapolation of the linear part until its intersection with the E_g axis provides the values of band gap.

For example: TiO_2

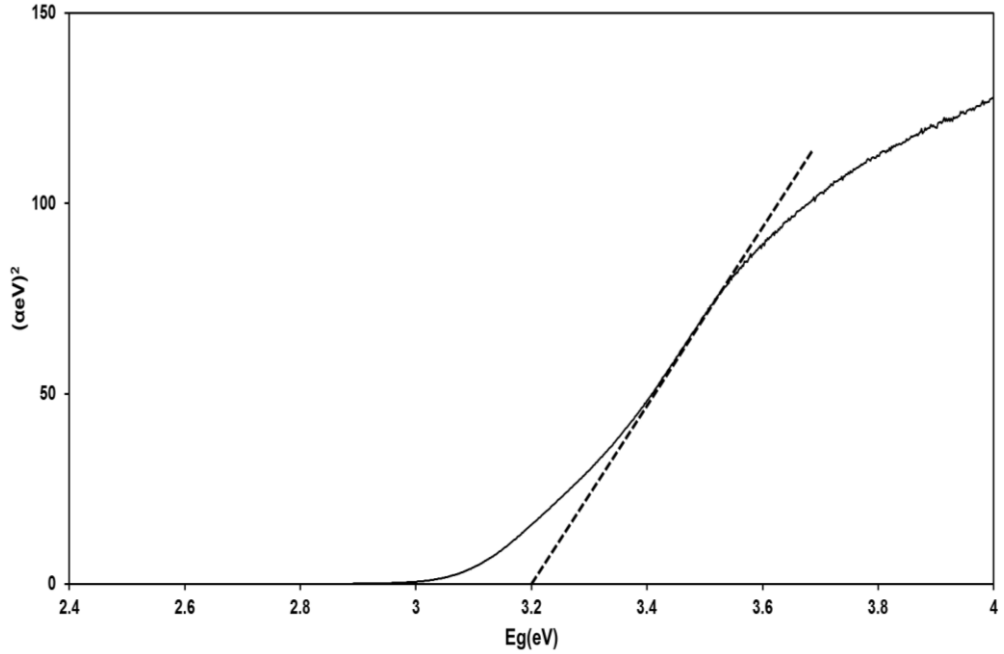

Figure H.1 Band gap energy of titanium dioxide

From the Figure H.1:

The band gap energy of TiO_2 = 3.2 eV

VITA

Miss. Kamonthip Tammarakwattana was born on September 19, 1993 in Chonburi province, Thailand. She received her Bachelor Degree of Chemical Engineering from Faculty of Engineering, King Mongkut Institute of Technology Ladkrabang, Thailand in 2016. She continued her Master study in the major in Chemical Engineering at Chulalongkorn University, Bangkok, Thailand in October 2016.

Kamonthip Tammarakwattana and Akawat sirisuk. Photocatalytic degradation of methylene blue over polydopamine-Ag/TiO2. Proceeding of pure and applied chemistry International conference, Prince of Songkla University, Hat Yai, Songkla, Thailand. Feb. 7-9, 2018 (PACCON 2018)